ASTRONOMY & ASTROPHYSICS
SUPPLEMENT SERIES

AUGUST 1990, PAGE 377

Astron. Astrophys. Suppl. Ser. **84**, 377-396 (1990)

Analysis of the light variations of the Wolf-Rayet star WR16(*)

E. Gosset([1]), J.-M. Vreux([2]), J. Manfroid([2])(**), M. Remy([3,2])(***) and C. Sterken([4])(**)

([1]) European Southern Observatory, Karl-Schwarzschild-Str., 2, D-8046 Garching bei München, Federal Republic of Germany
([2]) Institut d'Astrophysique, Université de Liège, avenue de Cointe, 5, B-4200 Cointe-Ougrée, Belgium
([3]) European Southern Observatory, La Silla, Chile
([4]) Astrophysical Institute, Vrije Universiteit Brussel, Pleinlaan, 2, B-1050 Brussel, Belgium

Received December 18, 1989; accepted January 31, 1990

Abstract. — New photometric data on the Wolf-Rayet star WR16 are presented and, together with already published data, are analyzed in detail. We show that WR16 is indeed variable, with dominating power at low frequencies ($\nu < 1.5\ d^{-1}$). We do not confirm the sudden brightness jumps reported by van Genderen, van der Hucht and Bakker (1989). The light variations are positively correlated for time lags up to two days. We present a simple stochastic model for the low frequency variability of the star that consists in a one-day step Moving Average process of order two. It is able to explain all the presently available observations and has the advantage of simplicity over a second, partially deterministic, model that is composed of a white-noise process and of two or three superimposed frequencies (respectively $\nu_A = 0.110\ d^{-1}$, $\nu_B = 0.066\ d^{-1}$, and perhaps $\nu_C = 0.183\ d^{-1}$, or their one-day aliases). Good evidence is also presented for the existence of a biperiodicity ($\nu_\alpha = 0.273\ d^{-1}$, $\nu_\beta = 0.376\ d^{-1}$ or their one day aliases) in one-of the comparison stars, HD86000.

Key words : stars: HD86161 — stars: HD86000 — stars: variable — stars: Wolf-Rayet — numerical methods.

1. Introduction.

WR16 (≡ HD86161, $V \sim 8.3$) is the second brightest known Wolf-Rayet star of subclass WN8. On the basis of extensive intermediate-band differential photometry, Moffat and Niemela (1982) reported its variability. The star was observed together with two comparison stars, namely HD86199 and HD86441 (notation: WR16/HD86199/HD86441). The latter however turned out to be variable (Moffat, 1977), and the final conclusions of Moffat and Niemela (1982) were based on the sole difference WR16 *minus* HD86199. A period search led to a periodicity $P = 5.365$ days. On the basis of various arguments, they adopted a $P = 10.73$ days double-wave lightcurve. The depths of the two minima were only marginally different. Spectroscopic data were also presented by Moffat and Niemela (1982); they supported the $P = 10.73$ days periodicity with a small K value of 6 km s^{-1}, which corresponds only to a 3σ level. Moffat and Niemela (1982) concluded that WR16 is an ellipsoidal variable with either a white dwarf or, more likely, a compact star as a companion.

More recently, van Genderen, van der Hucht and Steemers (1987) published some Walraven photometric measurements (WR16/HD86000). They pointed out that a phase diagram, constructed with Moffat and Niemela's (1982) ephemeris, exhibits a large intrinsic scatter.

At the same time, Lamontagne and Moffat (1987) presented new V, I differential photometry WR16/HD86199 /HD86118. HD86118 turned out to be an eclipsing variable, and they proposed a period $P = 1.78$ day. This star is well known under the name QX Carinae, an eclipsing binary with a period of 4.478 days (Strohmeier, Knigge and Ott, 1964; Cousins, Lagerweij and Shillington, 1969; Andersen *et al.*, 1983). Lamontagne and Moffat (1987) thus observed the primary minimum and also the secondary one, which is at phase 0.4. On the basis of their data, Lamontagne and Moffat (1987) proposed for WR16 a best period $P = 10.5$ days and concluded that the same kind of variation was visible over the ten year interval spent since Moffat and Niemela's (1982) observations. Finally, they remarked on the large scatter exhibited by the data points around the mean lightcurve.

Simultaneously, Manfroid, Gosset and Vreux (1987) presented Strömgren b differential photometry WR16 /HD86000/HD86199. They discovered that HD86199, an

(*) Based on observations collected at the European Southern Observatory (La Silla, Chile).
(**) Senior Research Associate, Belgian FNRS/NFWO.
(***) Also, Aspirant au Fonds National de la Recherche Scientifique (Belgium).

Ap star of type B9pSi, was variable with a period $P = 5.494$ days. The lightcurve was typical of this kind of star, and they demonstrated that HD86199 was responsible for the periodic variability attributed to WR16 by Moffat and Niemela (1982). They also found that their data WR16/HD86000 were well represented by two sines of frequencies $\nu = 0.744\ d^{-1}$ ($P = 1.344$ d) and $\nu = 0.392\ d^{-1}$ ($P = 2.551$ d). The data of van Genderen, van der Hucht and Steemers (1987), although not numerous, were also compatible with these frequencies, whereas the data of Moffat and Niemela (1982) -corrected for the variability of the Ap star-yield $\nu = 0.755\ d^{-1}$ ($P = 1.324$ d), a frequency already seen in the other datasets, and $\nu = 0.0765\ d^{-1}$ ($P = 13.1$ d). However, the latter results are to be taken with some caution because of the errors introduced by the above-mentioned manipulation. At this stage, WR16 is clearly not the simple binary claimed by Moffat and Niemela (1982), but the true nature of its variability remains unknown, essentially because most of the comparison stars were variable (for example, we note that the difference between the two minima in Figure 1 of Moffat and Niemela (1982) cannot be explained by the stable lightcurve of the Ap star).

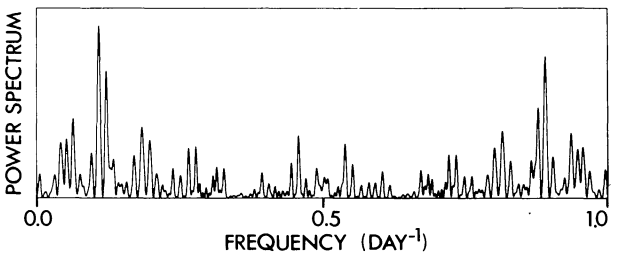

FIGURE 1. — Power spectrum (method of Deeming, 1975) of the Strömgren *b* filter differential magnitudes of WR16 corresponding to dataset Ia. The ordinates are in arbitrary units.

In order to help in clarifying this situation, we have analyzed the data of Lamontagne and Moffat (1987). After having removed the three measurements corresponding to an eclipse of HD86118, we have submitted each of the three sets of differential magnitudes WR16/HD86199/HD86118 to Fourier analysis. Table I presents the results for both filters and gives the frequency of the highest peak present in the power spectrum along with that of the second peak if it is higher than half the height of the first one. We see that a periodicity around $\nu \sim 0.19\ d^{-1}$ (~ 5 d) is most probably present and can be associated with HD86199. Such a result confirms the conclusions of Manfroid, Gosset and Vreux (1987). Table I is also suggestive of the presence of a periodicity of roughly 10 days associated with the Wolf-Rayet star, in rather good agreement with the suggestion of Lamontagne and Moffat (1987).

In order to test this and to further investigate the variability of WR16, we have collected new extensive datasets of Strömgren differential photometry. The first part of the data have been acquired at the European Southern Observatory as part of Sterken's Long-term Photometry of Variables project (Sterken, 1983), whereas the remaining parts have also been acquired at ESO during observing runs particularly dedicated to our project of investigating the variability of Wolf-Rayet stars.

TABLE I. — *Position of the peaks* (d^{-1}) *in the power spectrum of the modified data of Lamontagne and Moffat (1987).*

	V		I	
WR16–HD86199	0.096	0.185	0.104	0.204
WR16–HD86118	0.114		0.117	
HD86118–HD86199		0.185		0.177
	↑ WR16	↑ HD86199	↑ WR16	↑ HD86199

Preliminary results based on a subset of the first part have already been given by Gosset *et al.* (1989b): the variability of WR16 exhibits high power around a characteristic time scale of about 10 days, but the situation is more complex than just that. These conclusions are developed in the present paper. Recently, analyzing some of these same data, van Genderen, van der Hucht and Bakker (1989) reached the same conclusion. They also presented an interesting discussion on the colour variations of the star and on the relative importance of the emission-line and of the continuum contributions to the variability. In addition, they gave evidence for a jump in brightness of the Wolf-Rayet star ($|\Delta y| \sim 0.04$ mag., $|\Delta (u - v)| \sim 0.11$ mag.), an event which is similar to the one that took place in WR6 (van der Hucht, van Genderen and Bakker, 1990).

Finally, Balona and Egan (1989) and Balona, Egan and Marang (1989a, b) presented an extensive dataset of original Strömgren *b* filter differential photometry (WR16/HD88907/HD89104) made at the South African Astronomical Observatory. They showed that WR16 was indeed variable. They noticed a changing period on the time basis of their dataset ($\sim$ 120 days), and deduced a typical scale between 15-20 days, which led to a proposed quasi-periodicity of 17.54 days. After having subtracted a fitted sine-wave with this period, they found no other periodicity; however, the remaining scatter amounts to 0.016 mag. r.m.s., a value well above the expected noise level. In an attempt to reach a global view concerning the variability of WR16, we present hereafter the various new datasets of Strömgren differential photometry collected at ESO along with a detailed analysis.

2. Observations.

The new data presented here can be partitioned into three datasets. Dataset I corresponds to observations carried out as part of the Long-term Photometry of Variables project

(Sterken, 1983). They were made at ESO during several runs at the Danish 50cm telescope, which was equipped with a four-channel photometer especially designed for Strömgren photometry. The filter set used is system nr.4 of Manfroid and Sterken (1987) and the diaphragm is either 21″ or 30″ (diameter). One observation consists of the sequence C_1 VC_2 VC_2 VC_1 sky, where C_1 and C_2 are the comparison stars (HD86000 and HD85810, respectively) and V is the variable Wolf-Rayet star (WR16). Each individual measurement is made of short integrations totalling 10 to 30 seconds. Typically, one or two such sequences were performed every night. Because of their homogeneity, these data have been reduced as a whole using a procedure based on the method outlined by Manfroid (1985).

Dataset II is a composite of a small number of observations made either at the ESO 50cm or 1m telescopes. For run 7, the observation consists of a sequence C_1 C_2 V sky C_1 C_2 V sky C_1 C_2 V sky C_1 C_2 V sky C_1 C_2 V sky, each of the individual measurements corresponding to integrations totalling 40 to 60 seconds through a 30″ diaphragm. Concerning run 8, one observation consists of a short sequence V sky C_1 C_2, integrations reaching 40 to 70 seconds. The diaphragm used was 15″.5 during the first night and 10″.9 for subsequent ones.

The third dataset (III) corresponds to high precision observations carried out at ESO with the 1m telescope, equipped with a one-channel photometer. The filter used is ESO nr.324 alone, which corresponds to a Strömgren *b* filter and the diaphragm was 23″. One observation consists of the sequence C_3 C_1 C_2 V sky C_3 C_1 C_2 V sky C_3 C_1 C_2 V sky C_3 C_1 C_2 V sky where C_3 is a third comparison star (HD87419). Each individual measurement is made of short integrations totalling 30 to 100 seconds, and an entire sequence lasted between 30 and 45 minutes. Typically, some four such sequences were performed each night. The reduction procedure is the same as above. Of course, no colour transformation has been applied in the case of datasets II and III. Table II gives a summary and some more details on the observations.

The differential contemporaneous magnitudes $V-(C_1+C_2)/2$ computed as outlined by Manfroid (1985) are given in Table III for the first dataset. Data constituting dataset II are given in Table IV, whereas Table V contains the differential magnitudes $V-(C_1+C_2)/2$ as well as C_1-C_2 and C_1-C_3 relevant to dataset III.

TABLE II. — *Journal of the observations relevant to the new photometric data.*

Nr.	Run	JD(2440000+)	Telescope	Observer	Filter	N	Dataset
1	Dec 85	6412-6443	Danish 50cm	F.-J. Zickgraf*	uvby	50	Ia
2	Feb 86	6476-6496	Danish 50cm	M. Burger*	uvby	25	Ia
3	Mar 86	6498-6519	Danish 50cm	A. Jorissen*	uvby	28	Ia
4	Jun 86	6581-6589	Danish 50cm	H. Steenman*	uvby	8	Ia
5	Dec 87	7147-7162	Danish 50cm	Y.K. Ng*	uvby	12	Ib
6	Jan 88	7164-7180	Danish 50cm	E. Bibo*	uvby	30	Ib
7	Apr 88	7254-7254	ESO 50cm	M. Remy	b	1	II
8	Nov 88	7475-7495	Danish 50cm	M. Hiesgen*	uvby	20	Ib
9	Dec 88	7509-7513	ESO 1m	C. Sterken	b	5	II
10	Mar 89	7590-7616	Danish 50cm	E. Bibo*	uvby	48	Ib
11	Mar 89	7591-7598	ESO 1m	J. Manfroid	b	33	III

* Observer for the Long-term Photometry of Variables project.

3. Analysis of the data.

3.1 DATASET I. — A large gap occurs in the data coverage between run 4 and run 5. Therefore, we have decided to divide dataset I in two parts that will first be analyzed separately: they are indexed a and b (see Table II). The differential magnitudes relevant to each run have been averaged and the corresponding means and standard deviations are given in Table VI. Two measurements in run 10 presented a large deviation; they have therefore been rejected from any further treatment. They are given in parentheses in Table III. From Table VI, it is clear that the Wolf-Rayet star was varying. The variance is somewhat smaller for the *b* filter, this could be due to a spectral line effect (see also van Genderen, van der Hucht and Bakker, 1989).

It is obvious, from Table VI, that our data do not support the existence of the strong jump in brightness reported by van Genderen, van der Hucht and Bakker (1989). They remarked on a jump between run 3 and run 4. The difference for the *y* filter is non-existent in our data and certainly could not reach 0.04 mag. The jump in the colour $u-v$ is very small and can be attributed to a sampling fluctuation; it certainly does not reach the value of 0.11 mag. As the observations on which van Genderen, van der Hucht and Bakker (1989) rely, are the same than the ones analyzed here and as our resulting magnitudes diverge, we conclude that the more extensive datasets presented here permit a more accurate colour transformation. Such an improved transformation leads to more homogeneous magnitudes for the Wolf-Rayet star and jumps have disappeared. They are therefore not attributable to WR16 itself.

3.1.1 *Dataset Ia.* — Dataset Ia consists of 111 Strömgren *uvby* measurements. Data from each of the four filters have been independently analyzed in the frequency domain up to $\nu = 3\,\mathrm{d}^{-1}$ (day^{-1}) using Fourier techniques (Deeming, 1975; Scargle, 1982). The natural width of the peaks is $1/T \sim 0.006\,\mathrm{d}^{-1}$, where T is the total length in time of the dataset. We first point out that the power spectra relevant to the differential magnitudes $V-(C_1+C_2)/2$, $V-C_1$ and $V-C_2$ are virtually identical. We will use the first type. We also point out that the power spectra relevant to each filter are extremely similar indicating that the harmonic contents are only marginally wavelength dependent. As an example, Figure 1 gives the power spectrum (Deeming, 1975) relevant to the *b* filter. A peak clearly stands out at $\nu_1 = 0.109\,\mathrm{d}^{-1}$ ($P = 9.174$ d). If we model the variability with a sinusoid of the same frequency, an estimation of the relevant semi-amplitude a can be deduced either from the

TABLE III. — *Differential magnitudes V-(C_1 + C_2)/2 corresponding to dataset I as a function of the heliocentric julian date of observation and of the Strömgren filter utilized.*

HJD(2440000+)	u	v	b	y
6412.8216	0.1765	0.6666	0.2894	0.2379
6413.7955	0.1634	0.6637	0.2869	0.2373
6414.7950	0.1788	0.6669	0.2870	0.2384
6415.7161	0.1782	0.6758	0.3008	0.2491
6415.8190	0.1544	0.6559	0.2846	0.2312
6416.7357	0.1457	0.6413	0.2701	0.2127
6416.8152	0.1488	0.6431	0.2739	0.2143
6420.8050	0.1619	0.6593	0.2829	0.2244
6421.7509	0.1832	0.6841	0.3039	0.2550
6421.8204	0.1881	0.6830	0.3092	0.2592
6422.7366	0.1714	0.6691	0.2963	0.2441
6422.8171	0.1642	0.6649	0.2890	0.2342
6423.7199	0.1818	0.6794	0.2988	0.2456
6423.8291	0.1868	0.6773	0.2979	0.2518
6424.7095	0.1780	0.6755	0.2961	0.2503
6424.8227	0.1783	0.6702	0.2950	0.2458
6425.7232	0.1886	0.6856	0.2991	0.2581
6425.8333	0.1920	0.6874	0.3035	0.2658
6427.7254	0.2004	0.6995	0.3150	0.2702
6427.8346	0.2090	0.7014	0.3201	0.2764
6428.7026	0.1979	0.6900	0.3117	0.2649
6428.8369	0.1847	0.6783	0.3073	0.2549
6429.7072	0.1690	0.6629	0.2860	0.2375
6429.8354	0.1818	0.6755	0.2963	0.2552
6430.7105	0.1602	0.6560	0.2924	0.2367
6430.8336	0.1548	0.6448	0.2765	0.2174
6431.6971	0.1627	0.6547	0.2794	0.2194
6431.8467	0.1735	0.6643	0.2867	0.2389
6432.6863	0.1630	0.6643	0.2891	0.2331
6432.8467	0.1538	0.6537	0.2846	0.2288
6433.6849	0.1512	0.6497	0.2717	0.2230
6433.8426	0.1633	0.6590	0.2784	0.2373
6434.6871	0.1578	0.6539	0.2817	0.2371
6434.8399	0.1576	0.6510	0.2734	0.2306
6435.6781	0.1838	0.6790	0.2982	0.2565
6435.8392	0.1683	0.6661	0.2856	0.2454
6436.6781	0.1901	0.6863	0.3099	0.2612
6436.8390	0.1925	0.6849	0.3097	0.2660
6437.6847	0.1966	0.6909	0.3099	0.2663
6437.8379	0.1916	0.6918	0.3102	0.2679
6439.6894	0.1704	0.6725	0.2944	0.2537
6439.8421	0.1720	0.6742	0.2922	0.2514
6440.6792	0.1654	0.6638	0.2894	0.2350
6440.8418	0.1692	0.6665	0.2864	0.2377
6441.6821	0.1680	0.6655	0.2873	0.2388
6441.8451	0.1617	0.6624	0.2843	0.2420
6442.6832	0.1694	0.6682	0.2908	0.2429
6442.8373	0.1762	0.6727	0.2940	0.2526
6443.6797	0.2073	0.6943	0.3187	0.2710
6443.8277	0.1995	0.6978	0.3218	0.2666
6476.7155	0.1788	0.6691	0.2952	0.2371
6477.8181	0.1601	0.6617	0.2882	0.2370
6478.7285	0.1640	0.6618	0.2890	0.2328
6479.8451	0.1603	0.6595	0.2797	0.2401
6480.6135	0.1690	0.6675	0.2937	0.2469
6480.7844	0.1709	0.6646	0.2904	0.2434
6481.6635	0.1707	0.6697	0.2893	0.2424
6481.8002	0.1864	0.6786	0.3000	0.2560
6482.7076	0.1831	0.6816	0.3107	0.2516
6483.7647	0.1727	0.6700	0.2939	0.2459
6484.7587	0.1843	0.6735	0.3032	0.2529
6486.6886	0.1904	0.6798	0.3064	0.2420
6487.7461	0.1660	0.6536	0.2807	0.2196
6488.7344	0.1804	0.6740	0.3022	0.2408
6489.7205	0.1807	0.6745	0.3023	0.2431
6490.7499	0.1818	0.6727	0.3012	0.2425
6491.6723	0.2076	0.6970	0.3122	0.2676
6491.7975	0.1971	0.6866	0.3041	0.2582
6492.6982	0.1932	0.6876	0.3068	0.2631
6493.7435	0.1762	0.6736	0.2979	0.2471
6493.8197	0.1863	0.6812	0.3027	0.2525
6494.7042	0.1663	0.6633	0.2887	0.2395
6495.7134	0.1683	0.6619	0.2864	0.2316
6496.6521	0.1609	0.6634	0.2911	0.2438
6496.8127	0.1663	0.6650	0.2904	0.2392
6498.6537	0.1809	0.6712	0.2964	0.2459
6499.7483	0.2011	0.6821	0.3077	0.2476
6500.6820	0.1689	0.6662	0.2962	0.2458
6501.7021	0.1993	0.6899	0.3126	0.2726
6502.7155	0.2017	0.6895	0.3131	0.2621
6503.5869	0.2002	0.6806	0.3073	0.2580
6503.7179	0.1838	0.6793	0.3038	0.2582
6504.7036	0.1675	0.6642	0.2909	0.2388
6504.7719	0.1652	0.6672	0.2985	0.2531
6505.7257	0.1374	0.6434	0.2688	0.2127
6505.7769	0.1446	0.6424	0.2686	0.2113
6506.6049	0.1698	0.6624	0.2891	0.2410
6506.7868	0.1694	0.6665	0.2915	0.2525
6507.5517	0.1630	0.6646	0.2920	0.2524
6507.7554	0.1633	0.6637	0.2899	0.2474
6508.7185	0.1808	0.6828	0.3091	0.2582
6509.6553	0.1802	0.6746	0.3034	0.2360
6509.7478	0.1667	0.6580	0.2876	0.2258
6510.6758	0.1705	0.6677	0.2935	0.2450
6511.6482	0.1758	0.6639	0.2969	0.2347
6512.6703	0.1825	0.6705	0.2976	0.2456
6513.6821	0.2013	0.6865	0.3053	0.2671
6516.7032	0.1709	0.6562	0.2840	0.2325
6517.6755	0.1882	0.6771	0.3019	0.2533
6518.6017	0.1899	0.6773	0.3048	0.2549
6518.7556	0.2252	0.7045	0.3240	0.2712
6519.6462	0.2009	0.6916	0.3185	0.2676
6519.7690	0.1922	0.6841	0.3124	0.2572
6581.4880	0.1466	0.6442	0.2768	0.2216
6582.4913	0.1976	0.6943	0.3184	0.2740
6583.5147	0.1678	0.6689	0.2935	0.2405
6584.4769	0.1668	0.6679	0.2940	0.2468
6585.4720	0.1686	0.6699	0.2939	0.2530
6587.4827	0.1641	0.6647	0.2930	0.2473
6588.5081	0.1475	0.6453	0.2778	0.2193
6589.4800	0.1717	0.6734	0.3043	0.2603

TABLE III (*continued*)

HJD(2440000+)	u	v	b	y	HJD(2440000+)	u	v	b	y
7147.8380	0.1887	0.6856	0.3097	0.2664	7489.7640	0.1464	0.6493	0.2772	0.2204
7148.8298	0.1669	0.6694	0.2985	0.2543	7490.7605	0.2153	0.7027	0.3218	0.2875
7150.8405	0.1755	0.6607	0.2869	0.2279	7491.7462	0.1988	0.7001	0.3217	0.2790
7151.8322	0.1563	0.6573	0.2854	0.2354	7492.7522	0.1973	0.6944	0.3182	0.2744
7152.8215	0.1685	0.6672	0.2913	0.2462	7493.7454	0.2167	0.6961	0.3200	0.2771
7155.7981	0.1959	0.6928	0.3194	0.2784	7494.7636	0.1746	0.6692	0.2979	0.2373
7156.8283	0.1946	0.6891	0.3121	0.2729	7495.7440	0.1703	0.6662	0.2890	0.2441
7158.8036	0.1796	0.6771	0.3024	0.2549	7590.7632	(0.3441)	(0.7727)	(0.3776)	(0.2930)
7159.7707	0.1544	0.6545	0.2899	0.2348	7591.7316	0.1603	0.6539	0.2843	0.2376
7160.7634	0.1743	0.6770	0.3007	0.2577	7592.5652	0.1628	0.6682	0.3030	0.2555
7161.8170	0.1627	0.6580	0.2836	0.2254	7592.6596	0.1720	0.6669	0.2927	0.2337
7162.8078	0.1394	0.6363	0.2705	0.2156	7593.5517	0.1489	0.6496	0.2813	0.2335
7164.7648	0.1608	0.6654	0.2904	0.2503	7594.5830	0.1763	0.6664	0.2919	0.2439
7165.7372	0.1763	0.6701	0.3007	0.2493	7594.6928	0.1664	0.6648	0.2933	0.2470
7166.6954	0.1581	0.6593	0.2850	0.2374	7595.6085	0.1956	0.6887	0.3058	0.2671
7167.7431	0.1757	0.6717	0.3028	0.2448	7595.7213	0.1889	0.6818	0.3019	0.2635
7167.8059	0.1707	0.6693	0.2974	0.2444	7596.5606	0.1587	0.6573	0.2863	0.2341
7168.6747	0.1785	0.6773	0.2986	0.2574	7596.7288	0.1699	0.6672	0.2907	0.2446
7168.8055	0.1740	0.6767	0.3002	0.2661	7597.5481	0.1721	0.6732	0.3020	0.2577
7169.6848	0.1880	0.6894	0.3148	0.2665	7597.7108	0.1783	0.6696	0.2985	0.2479
7169.7995	0.2018	0.6961	0.3231	0.2779	7598.6105	0.1518	0.6480	0.2836	0.2220
7170.7014	0.1984	0.6964	0.3272	0.2677	7598.7162	0.1454	0.6442	0.2770	0.2176
7171.7367	0.1704	0.6658	0.2906	0.2414	7599.5837	0.1746	0.6683	0.2922	0.2507
7171.8307	0.1637	0.6648	0.2904	0.2504	7599.7313	0.1831	0.6749	0.2990	0.2570
7172.7331	0.1688	0.6659	0.2915	0.2451	7600.5543	0.1769	0.6772	0.3003	0.2567
7172.8196	0.1753	0.6716	0.3010	0.2483	7600.7846	0.1696	0.6745	0.3028	0.2620
7173.7436	0.1797	0.6802	0.3075	0.2589	7601.5999	0.1723	0.6743	0.3013	0.2474
7173.8189	0.1797	0.6812	0.3072	0.2566	7601.7136	0.1672	0.6651	0.2985	0.2418
7174.7222	0.1825	0.6852	0.3049	0.2598	7602.5330	0.1656	0.6652	0.2987	0.2348
7174.8422	0.1935	0.6874	0.3118	0.2644	7602.6973	0.1562	0.6538	0.2853	0.2200
7175.7321	0.2012	0.6968	0.3214	0.2717	7603.5757	0.1651	0.6632	0.2871	0.2377
7175.8455	0.1985	0.6953	0.3242	0.2735	7603.7499	0.1668	0.6639	0.2895	0.2369
7176.7415	0.1646	0.6643	0.2921	0.2385	7605.6268	0.1776	0.6679	0.2898	0.2398
7176.8504	0.1580	0.6571	0.2828	0.2352	7605.7440	0.1682	0.6655	0.2906	0.2408
7177.7370	0.1703	0.6635	0.2867	0.2458	7606.5795	0.1642	0.6611	0.2859	0.2438
7177.8485	0.1743	0.6730	0.2957	0.2573	7606.7439	0.1660	0.6572	0.2805	0.2363
7178.7361	0.1720	0.6678	0.2959	0.2503	7607.5662	0.1784	0.6721	0.2954	0.2451
7178.8542	0.1745	0.6759	0.3025	0.2622	7607.7272	(0.2400)	(0.7327)	(0.3645)	(0.3240)
7179.7348	0.1703	0.6686	0.2949	0.2425	7608.5857	0.1341	0.6324	0.2685	0.2091
7179.8492	0.1766	0.6752	0.3007	0.2598	7608.7146	0.1390	0.6376	0.2710	0.2198
7180.7286	0.1789	0.6827	0.3058	0.2630	7609.5581	0.1777	0.6735	0.2995	0.2511
7180.8534	0.1816	0.6789	0.3081	0.2668	7610.5774	0.1674	0.6636	0.2921	0.2389
7475.8309	0.1997	0.6929	0.3161	0.2634	7610.6925	0.1531	0.6508	0.2818	0.2314
7476.8004	0.1861	0.6900	0.3124	0.2705	7611.5538	0.1899	0.6890	0.3127	0.2695
7477.8058	0.1631	0.6630	0.2864	0.2394	7611.6948	0.1834	0.6818	0.3059	0.2626
7478.7904	0.1799	0.6672	0.2918	0.2381	7612.5936	0.1786	0.6760	0.3003	0.2560
7479.7784	0.1772	0.6726	0.2940	0.2427	7612.7221	0.1814	0.6761	0.3002	0.2597
7480.7852	0.1769	0.6807	0.2984	0.2526	7613.5574	0.1999	0.6969	0.3245	0.2786
7481.7771	0.1816	0.6746	0.3038	0.2457	7613.7068	0.1826	0.6835	0.3080	0.2598
7482.7783	0.1994	0.6922	0.3172	0.2755	7614.5691	0.1811	0.6793	0.3017	0.2506
7483.8352	0.1721	0.6609	0.2935	0.2276	7614.7451	0.1958	0.6904	0.3092	0.2600
7484.7782	0.1819	0.6777	0.3034	0.2525	7615.5925	0.1728	0.6687	0.2976	0.2390
7486.7746	0.1717	0.6606	0.2948	0.2277	7615.7192	0.1650	0.6643	0.2948	0.2388
7487.7882	0.1868	0.6714	0.3012	0.2383	7616.5549	0.1717	0.6767	0.3034	0.2618
7488.7607	0.1584	0.6562	0.2805	0.2319	7616.7207	0.1759	0.6709	0.2935	0.2418

TABLE IV. — *Differential magnitudes V-(C_1+C_2)/2 (Strömgren b filter) corresponding to dataset II.*

HJD(2440000+)	*b*
7254.7047	0.3009
7509.7745	0.2639
7510.7852	0.2627
7511.7690	0.2719
7512.7478	0.2993
7513.7909	0.2749

TABLE V. — *Differential magnitudes (Strömgren b filter) V-(C_1+C_2)/2, C_1-C_2 and C_1-C_3 corresponding to dataset III.*

HJD(2440000+)	V-(C_1+C_2)/2	HJD(2440000+)	C_1-C_2	C_1-C_3
7591.5437	0.2627			
7591.5710	0.2643	7591.5587	0.2090	−0.2912
7591.6480	0.2650	7591.6534	0.2098	−0.2932
7591.7364	0.2583	7591.7434	0.2084	−0.2937
7591.8221	0.2590	7591.8294	0.2086	−0.2933
7592.5381	0.2664	7592.5446	0.2091	−0.2937
7592.6315	0.2633	7592.6380	0.2098	−0.2938
7592.7233	0.2661	7592.7290	0.2083	−0.2939
7592.8028	0.2662	7592.8082	0.2095	−0.2923
7593.5421	0.2537	7593.5476	0.2072	−0.2959
7593.6213	0.2503	7593.6265	0.2101	−0.2926
7593.7054	0.2550	7593.7106	0.2100	−0.2917
7593.8040	0.2560	7593.8106	0.2119	−0.2921
7594.5882	0.2613			
7594.6123	0.2671	7594.5940	0.2099	−0.2924
7594.6698	0.2682	7594.6755	0.2133	−0.2932
7594.7599	0.2728	7594.7658	0.2024	−0.2966
7595.5491	0.2808	7595.5551	0.2087	−0.2932
7595.6261	0.2770	7595.6322	0.2079	−0.2922
7595.7097	0.2772	7595.7183	0.2096	−0.2923
7595.7994	0.2686	7595.8053	0.2085	−0.2917
7596.5526	0.2620	7596.5582	0.2109	−0.2944
7596.6113	0.2612	7596.6166	0.2107	−0.2931
7596.6830	0.2612	7596.6883	0.2114	−0.2937
7596.7543	0.2718	7596.7600	0.2107	−0.2910
7597.5323	0.2816	7597.5342	0.2094	−0.2942
7597.6137	0.2732	7597.6194	0.2089	−0.2938
7597.6822	0.2746	7597.6875	0.2093	−0.2946
7597.7722	0.2755	7597.7775	0.2105	−0.2937
7598.5409	0.2569	7598.5484	0.2098	−0.2912
7598.6028	0.2522	7598.6084	0.2079	−0.2916
7598.6729	0.2484	7598.6787	0.2081	−0.2911
7598.7459	0.2517	7598.7518	0.2068	−0.2933

TABLE VI. — *Means (above) and standard deviations (below) of the differential magnitudes corresponding to each run contained in dataset I.*

V-(C_1+C_2)/2

Run or Dataset	*u*	*v*	*b*	*y*
1	0.1748	0.6709	0.2939	0.2454
	0.0157	0.0150	0.0130	0.0158
2	0.1769	0.6717	0.2963	0.2447
	0.0124	0.0102	0.0089	0.0103
3	0.1801	0.6724	0.2988	0.2482
	0.0189	0.0142	0.0130	0.0154
4	0.1663	0.6661	0.2940	0.2454
	0.0159	0.0160	0.0134	0.0184
5	0.1714	0.6688	0.2959	0.2475
	0.0170	0.0165	0.0139	0.0199
6	0.1772	0.6758	0.3018	0.2551
	0.0120	0.0113	0.0118	0.0115
8	0.1827	0.6769	0.3020	0.2513
	0.0179	0.0159	0.0140	0.0201
10	0.1706	0.6677	0.2946	0.2453
	0.0140	0.0134	0.0107	0.0148
Ia	0.1760	0.6711	0.2957	0.2459
	0.0161	0.0138	0.0122	0.0147
Ib	0.1748	0.6718	0.2981	0.2494
	0.0152	0.0141	0.0124	0.0161
I	0.1754	0.6714	0.2969	0.2476
	0.0156	0.0139	0.0123	0.0154

C_1-C_2

Dataset	*u*	*v*	*b*	*y*
Ia	0.3738	0.2554	0.2121	0.1882
	0.0049	0.0030	0.0032	0.0033
Ib	0.3730	0.2551	0.2112	0.1874
	0.0053	0.0037	0.0034	0.0041
I	0.3734	0.2553	0.2117	0.1878
	0.0051	0.0033	0.0033	0.0037

power of the peak or from a least-squares fit to the data. The semi-amplitudes are about 0.01 mag., and the detailed results for each filter are given in the first lines of Table VII.

The presence of a peak in a power spectrum is not necessarily due to the existence of a periodicity. For example, the peak could just appear as a random fluctuation of stochastic variations (e.g. a white-noise process). In order to be sure that we have to deal with an at least partially deterministic process, we have to apply a statistical test. A convenient method is to adopt a white-noise process as a null-hypothesis and then to use the normalized power spectrum introduced by Scargle (1982) to compute (as a statistic) the normalized power P_N (power over variance) of the highest peak. The normalized powers associated with $\nu_1 = 0.109\,d^{-1}$ are also given in Table VII. The higher the peak is, the stronger is the rejection of the null-hypothesis. Scargle (1982) has proposed a formula to compute the significance level corresponding to the highest peak (i.e. the probability under the null-hypothesis to have at least such a power in the peak). The significance level is, in his case, a function of the power of the peak and of the number of points constituting the observations. This is clearly an approximation; Horne and Baliunas (1986) have shown that the relevant probability law is also highly dependent on the temporal distribution of the measurements. Effectively, the sampling being uneven, correlations exist between the values of the power spectrum at different frequencies. Such correlations have some influence on the apparent number of degrees of freedom (Scargle, 1982). We cannot get rid of this effect by a simple analytical correction. Therefore, we have computed the corrected significance level by performing a large number of simulations (at least 2500). Each simulation consists in creating a dataset identical, with respect to the temporal distribution of the measurements, to the one studied here. But, each magnitude has been replaced by a random number drawn out of a Gaussian white-noise process with a dispersion similar to the one of the actual data. For each simulated dataset, we have searched for the highest peak in the power spectrum between 0.0 and 0.5 d^{-1} and have retained the corresponding value P_N. The distribution of the resulting P_N values over the simulations is a good approximation of the actual statistical distribution of the P_N's under the null-hypothesis. The comparison of the observed P_N values of Table VII with the derived statistical law permits the computation of a corrected significance level. It is also possible to fit the actual distribution of the P_N's under the null-hypothesis with a formula identical to the one given by Scargle (1982) but with the number of degrees of freedom N no longer assumed equal to $N_0/2$ (where N_0 is the number of observations) but instead considered as a free parameter of this fit. Such a fit gives a good approximation. The formula can then be used to compute the corrected significance level (CSL) as a function of the observed normalized power. The approach we just described permits the partial elimination of another problem. When computing Scargle's (1982) statistic, we have to oversample the power spectrum in order to assure a good evaluation of the phase correction factor $\tau(\omega)$. The oversampling implies that we are resolving the peaks in the power spectrum and, consequently, we always observe their apices. This situation is fundamentally different from the one corresponding to the classical approach for even sampling. The method described above furnishes a fair approximation for the correction of the oversampling. The CSL's are also given in Table VII. They are small and, as a conclusion, we can say that the null-hypothesis is strongly rejected and that therefore some deterministic process plays a role. The deviation from the null-hypothesis is towards the existence of a periodicity.

TABLE VII. — *Some details on the possible frequencies detected in dataset Ia (Symbols are explained in section 3.1.1).*

		u	v	b	y
$\nu_1 = 0.109\ d^{-1}$	a	0.0120	0.0102	0.0094	0.0103
	σ_a	0.0018	0.0016	0.0014	0.0017
	P_N	15.3	14.9	16.5	13.5
	CSL	0.00004	0.00005	0.00002	0.0002
	NSL	0.001	0.006	0.003	0.037
$\nu_2 = 0.066\ d^{-1}$	a	0.0101	0.0080	0.0066	0.0077
	σ_a	0.0016	0.0014	0.0013	0.0016
	P_N	14.3	12.2	10.8	9.5
	CSL	0.0001	0.0008	0.0031	0.0118
	NSL	0.001	0.014	0.001	0.078
$\nu_3 = 0.185\ d^{-1}$	a	0.0063	0.0059	0.0053	0.0057
	σ_a	0.0015	0.0013	0.0011	0.0015
	P_N	8.2	9.1	9.4	7.7
	CSL	0.0411	0.0171	> 0.01	0.0695
	NSL	> 0.10	> 0.10	> 0.10	> 0.10

The data of dataset Ia have been prewhitened (see Gosset *et al.*, 1989a, for an explanation of this term) for the frequency $\nu_1 = 0.109\,d^{-1}$, and analyzed again using the same technique as above. The data from each filter exhibit, in their power spectrum, a highest peak at $\nu_2 = 0.066\,d^{-1}$. Figure 2 gives, as an example, the power spectrum relevant to the b filter; the peak is still more outstanding for filters u and v. The details concerning ν_2 are given in the following part of Table VII. Although the situation is less straightforward for filter y, we can conclude that these data strongly suggest the existence of a second periodicity ν_2. The frequency ν_2 cannot be directly linked to the frequency ν_1; it should however be pointed out that the sampling of dataset Ia exhibits a strong aliasing at $\Delta\nu \sim 0.013\,d^{-1}$. As a consequence, the correct value for ν_2 could perhaps be $\nu_2 - \Delta\nu \sim 0.053\,d^{-1}$ and two times this value is not significantly different from ν_1 : so we cannot reject the idea that one is the harmonic of the other, although this is unlikely.

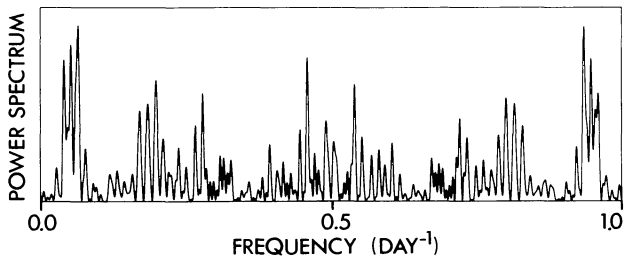

FIGURE 2. — Same as Figure 1 but corresponding to the differential magnitudes of dataset Ia prewhitened for the frequency ν_1=0.109 d^{-1}.

The data from dataset Ia prewhitened for the frequency ν_1 have again been prewhitened, this time for the frequency ν_2, and the resulting dataset has been analyzed. A peak is clearly visible for each of the four filters. It is situated at $\nu_3 = 0.185\,\mathrm{d}^{-1}$ ($P = 5.405$ d) and dominates in the power spectrum of the u and of the v filter data. The power spectrum corresponding to filter b is given in Figure 3. One can see the relevant peak at ν_3 but the dominant one is situated at $\nu = 0.460\,\mathrm{d}^{-1}$ ($P = 2.174$ d). This discrepancy is just a sign that we are reaching the "noise" level. The dominant peak for filter y is situated at $\nu = 0.172\,\mathrm{d}^{-1}$ ($P = 5.814$ d) and is an alias ($\Delta\nu \sim 0.013\,\mathrm{d}^{-1}$) of ν_3. Despite the slight discrepancy exhibited by the data from the filter b, we can adopt ν_3 as a third frequency possibly present in the variability of WR16. Table VII also gives, in the usual format, further details on ν_3. The significance levels are interestingly small but not enough to allow the rejection of the null-hypothesis. We are reaching here the level for the semi-amplitudes of about 0.006 mag. and, as will be explained in section 6, it is safer not going beyond this limit. We are also reaching the approximate level where no peak can safely be considered as significant. Therefore, we will have to stop here the detailed investigation of dataset Ia. In order to ascertain our results, we have nevertheless prewhitened the data for the frequency ν_3. The resulting datasets have standard deviations of $\sigma_u = 0.0108$, $\sigma_v = 0.0095$, $\sigma_b = 0.0083$ and $\sigma_y = 0.0108$, well above the observational noise ($\sigma = 0.0049$, 0.0030, 0.0032 and 0.0033 respectively, see Table VI) suggesting that the variability of the star is still making a large contribution. The power spectra of the new data exhibit several insignificant peaks. As three frequencies have already been removed from these data, it is not surprising that peaks seem to appear in the power spectrum by contrast with the frequency zones that have been cleaned. One can notice peaks at $\nu = 0.460\,\mathrm{d}^{-1}$ (filters u, v, b, y), $\nu = 0.280\,\mathrm{d}^{-1}$ (filters v, b, y), $\nu = 0.203\,\mathrm{d}^{-1}$ (filters u, v, y) and at low frequencies $\nu = 0.047\,\mathrm{d}^{-1}$ (filter u), $\nu = 0.059\,\mathrm{d}^{-1}$ (filter v), $\nu = 0.060\,\mathrm{d}^{-1}$ (filter b) and at $\nu = 0.073\,\mathrm{d}^{-1}$ (filter y). Only the peak relevant to the filter b at $\nu = 0.460\,\mathrm{d}^{-1}$ can be considered as slightly significant ($P_N \sim 10$, CSL ~ 0.01).

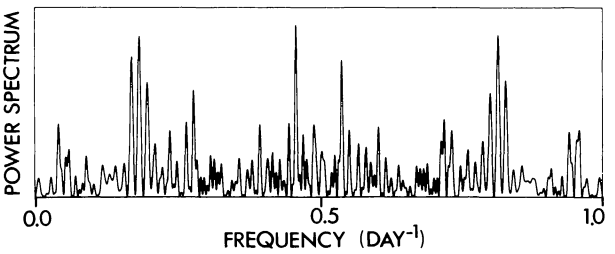

FIGURE 3. — Same as Figure 1 but corresponding to the differential magnitudes of dataset Ia prewhitened for the frequencies $\nu_1 = 0.109\,\mathrm{d}^{-1}$ and $\nu_2 = 0.066\,\mathrm{d}^{-1}$.

In order to further strengthen our conclusions, we have analyzed the different datasets with other types of method. Namely, we used the trial period methods of Lafler and Kinman (1965), Renson (1978) and Stellingwerf (1978). We will not detail this part of our work but we can essentially state that these different methods confirm our results obtained by the Fourier analysis. They also provide us with the opportunity to compute a significance level independent of the CSL. The method has been introduced by Nemec and Nemec (1985) and consists in estimating the null-hypothesis by randomizing the individual measurements among the times of observation. For each randomized dataset, the extremum of the statistic (in the present case, we used the Lafler and Kinman's (1965) one) is spotted and a distribution of the extrema under the null-hypothesis of white-noise is thus derived on the basis of several simulations. The observed extremum is then compared to this distribution and a significance level (noted NSL) can be derived. The NSL's are also given in Table VII: they are systematically larger than the CSL's but the above-mentioned conclusions are unchanged.

3.1.2 *Dataset Ib.* — Dataset Ib consists of 110 *uvby* measurements but two of them (within parentheses in Table III) have been rejected because they are doubtful. The natural width relevant to these observations is $1/T \sim 0.002\,\mathrm{d}^{-1}$. The power spectrum relevant to the b filter is given in Figure 4. A peak at $\nu_1 = 0.183\,\mathrm{d}^{-1}$ ($P = 5.464$ d) is slightly dominating. The power spectrum corresponding to the v filter is very similar, whereas, in the case of the y filter, the peak is clearly outstanding. The case of the u filter is more complicated because, although the peak at ν_1 is visible, another peak at $\nu = 0.116\,\mathrm{d}^{-1}$ ($P = 8.621$ d) is the highest one. The detailed results are given in Table VIII following the scheme of Table VII. The reported significance levels do not allow us to conclude that there exists any deterministic process. The use of the methods of Lafler and Kinman (1965) and of Renson (1978) confirms the difficulty to identify a particular frequency, although

the relevant periodograms exhibit insignificant dips around $\nu \sim 0.06\ d^{-1}$ and around $\nu \sim 0.11\ d^{-1}$. On the other hand, Stellingwerf's (1978) method locates two frequencies, the strongest one around $\nu \sim 0.10\ d^{-1}$, the other being around $\nu \sim 0.183\ d^{-1}$. The discrepancies between the results of the different methods utilized here are indicative that we are only dealing with marginal, insignificant effects.

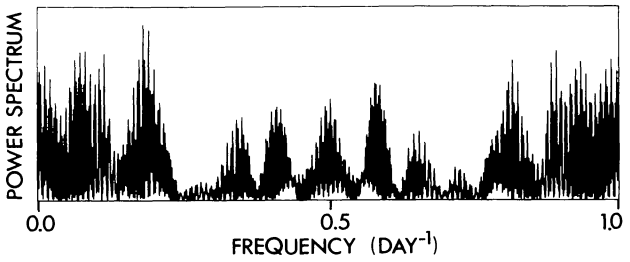

FIGURE 4. — Same as Figure 1 but corresponding to the differential magnitudes of dataset Ib.

TABLE VIII. — *Some details on the possible frequencies detected in dataset Ib.*

		u	v	b	y
$\nu_1 = 0.183\ d^{-1}$	a	0.0070	0.0077	0.0067	0.0090
	σ_a	0.0020	0.0018	0.0016	0.0020
	P_N	-	8.1	7.9	8.6
	CSL	-	0.0782	0.0965	0.0487
$\nu = 0.116\ d^{-1}$	a	0.0079			
	σ_a	0.0019			
	P_N	7.2			
	CSL	0.1883			

The data have been prewhitened for the frequency ν_1 or the frequency $\nu = 0.116\ d^{-1}$, and analyzed again. No peak is markedly outstanding in the new relevant power spectra. However, one can notice an excess of power between $\nu = 0.050\ d^{-1}$ and $\nu = 0.075\ d^{-1}$.

From dataset Ib, it is clear that no significant periodicity can be extracted. Nevertheless, three characteristic time scales can be suggested; they are represented by frequencies $\nu_1 = 0.183\ d^{-1}$, $\nu \sim 0.116\ d^{-1}$ and ν around $0.06\ d^{-1}$. It is interesting to notice that these three frequencies are in complete agreement with the ones deduced from dataset Ia in section 3.1.1.

3.1.3 *The whole dataset I.* — In this section, we will analyze dataset I that results from the merging of datasets Ia and Ib. The total number of measurements is 219; they are distributed between December 1985 and March 1989, corresponding to a natural width $1/T \sim 0.0008\ d^{-1}$. The power spectrum of the b filter data is given in Figure 5. It is representative of the power spectra corresponding to the other filters. The relative lack of power at low frequencies ($\nu < 0.020\ d^{-1}$) is suggestive of the long-term stability of the brightness of the star but also of the good quality of the photometry used here. The explored frequency domain goes from $0.0\ d^{-1}$ to $4.0\ d^{-1}$. The one-day aliasing is rather strong and the related ambiguity could not be resolved. The frequencies quoted here correspond to the alias situated between $0.0\ d^{-1}$ and $0.5\ d^{-1}$. Figure 5 clearly exhibits a peak at $\nu_1 = 0.110\ d^{-1}$ ($P = 9.091$ d). Once the data have been prewhitened for this frequency, another peak at $\nu_2 = 0.066\ d^{-1}$ ($P = 15.15$ d) appears in the power spectrum (see Figure 6 for the case of the b filter). The data have also been prewhitened for ν_2; Figure 7 gives the power spectrum of the resulting dataset as usual for the b filter. Clearly, a frequency $\nu_3 = 0.183\ d^{-1}$ ($P = 5.464$ d) is again present. Finally, the data have been prewhitened for ν_3 and the resulting data lead to power spectra that are nicely flat, free of any outstanding peak. This indicates that the resulting data are quite compatible with a white-noise process. The residual standard deviations are $\sigma_u = 0.0123$, $\sigma_v = 0.0108$, $\sigma_b = 0.0095$ and $\sigma_y = 0.0126$, i.e. well beyond the observational errors (see Table VI) indicating that a stochastic process also takes place in the star. The summary of the above results is given in Table IX in a scheme identical to the one of Table VII. It is interesting to note that, from filter to filter, the semi-amplitudes as well as the residual standard deviations are roughly in the same ratio, the smallest variability corresponding to the b filter.

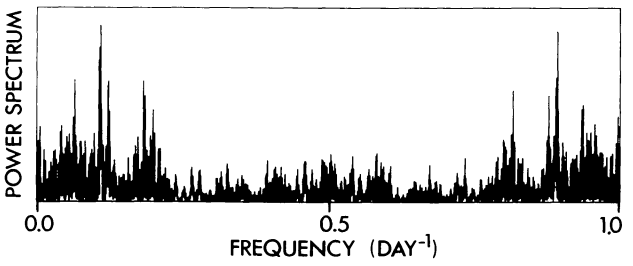

FIGURE 5. — Same as Figure 1 but corresponding to the differential magnitudes of dataset I.

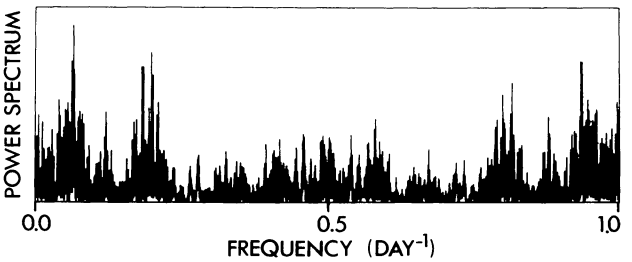

FIGURE 6. — Same as Figure 1 but corresponding to the differential magnitudes of dataset I prewhitened for the frequency $\nu_1 = 0.110\ d^{-1}$.

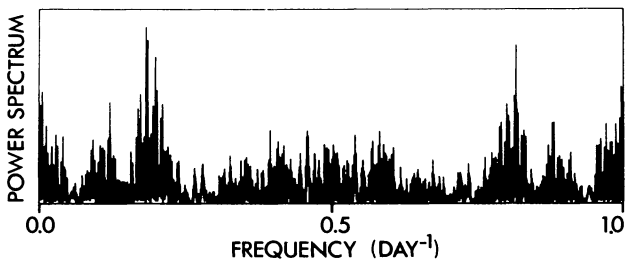

FIGURE 7. — Same as Figure 1 but corresponding to the differential magnitudes of dataset I prewhitened for the frequencies $\nu_1 = 0.110\,\mathrm{d}^{-1}$ and $\nu_2 = 0.066\,\mathrm{d}^{-1}$.

Stellingwerf's (1978) method has also been used to analyze the data. The conclusions are strictly identical to the above results, which is not surprising as both methods are strongly related (see e.g. Swingler, 1989). However, the methods of Lafler and Kinman (1965) and of Renson (1978) lead to periodograms where no particular frequencies can be easily picked out. This is directly understood if we recall that these methods are not good at finding multiperiodicities and if we further note that the possible deterministic process could be drowned in a stochastic one (see the above quoted residual standard deviations).

As Loumos and Deeming (1978) have demonstrated that the positions of the peaks in the power spectrum of a multiperiodic process could be non representative of the actual frequencies, we have made non-linear least-squares fits to the data with two or three frequencies. The resulting values are identical to the ones given in Table IX.

Although the inspection of Table IX reveals the existence of three significant frequencies, one should be cautious because the relevant quoted semi-amplitudes are extremely small. In fact, they are smaller than in Table VII, thereby underlining their statistical nature. The fact that merging dataset Ib with dataset Ia does not maintain the same values

TABLE IX. — *Some details on the possible frequencies detected in dataset I.*

		u	*v*	*b*	*y*
$\nu_1 = 0.110\ \mathrm{d}^{-1}$	a	0.0087	0.0076	0.0072	0.0076
	σ_a	0.0014	0.0012	0.0011	0.0014
	P_N	17.2	16.5	18.6	15.3
	CSL	0.00010	0.00020	0.00002	0.00067
$\nu_2 = 0.066\ \mathrm{d}^{-1}$	a	0.0078	0.0072	0.0062	0.0072
	σ_a	0.0013	0.0011	0.0010	0.0013
	P_N	16.3	17.2	16.6	13.4
	CSL	0.00025	0.00010	0.00019	0.00458
$\nu_3 = 0.183\ \mathrm{d}^{-1}$	a	0.0066	0.0067	0.0055	0.0070
	σ_a	0.0012	0.0010	0.0009	0.0012
	P_N	13.9	17.9	15.9	15.3
	CSL	0.00284	0.00005	0.00039	0.00022

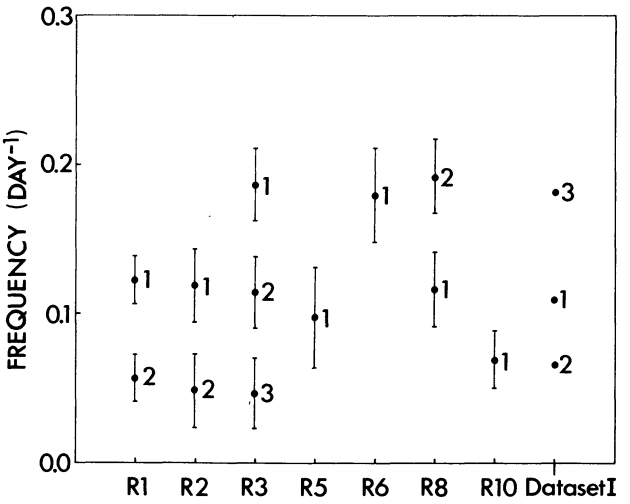

FIGURE 8. — Positions in the frequency domain of the most important peaks in the power spectrum of the Strömgren *b* filter differential magnitudes corresponding to each individual run (Run 1, Run 2,...) constituting dataset I. The error bars represent the natural width of the peaks. The peaks are labelled by an ordinal number.

of the semi-amplitudes, suggests that dataset Ib gives only little support to these frequencies. In order to further investigate the reality of the three frequencies, we have analyzed separately each convenient run and spotted the highest peaks in the power spectra. Figure 8 illustrates the positions of these peaks for the *b* filter magnitudes. It is immediately clear that each individual run supports the existence of the frequencies on the time scale of a dataset or more. In addition, the computation of the Completeness-of-Phase statistic introduced by McCandliss (1988) indicates that none of the observed frequencies can be an artifact of the sampling.

3.2 DATASETS II AND III. — Dataset II is too small to be of interest by itself and will only be used later. Dataset III is constituted of 33 *b* filter measurements distributed over 8 nights. It has a multiple purpose. First, a third star has been added in the sequence in order to check the stability of the comparison stars. This problem will be dealt with in section 6. The second thing we wanted to check concerns the effect of the presence of the visual companion. Effectively, WR16 has a visual companion some 8" away. Moffat and Niemela (1982) report that Johnson photometric observations of this companion lead to $V = 11.85$, $B = 12.75$. During run 11, the companion has been observed alone through a smaller diaphragm and we estimate for it a magnitude $b = 12.47$. Such a value is in good agreement with the Johnson magnitudes given above and is the proof of the stability of the companion over the 14 years spanned by the data. No problem is to be expected on this side. However, a problem could arise if the companion is not systematically maintained within

the diaphragm. The effect on the measured magnitude of WR16 of removing or not the companion from the diaphragm could amount to 0.025 mag., an amplitude far beyond what we are looking for. The companion is clearly visible at the 1m telescope but could be harder to detect at a 50cm telescope. Normally, the diaphragm used in the framework of the Long-term Photometry of Variables project should always be wide enough. As some of the data of run 11 are simultaneous with a part of run 10, we can thus check for this. The magnitudes of run 11 have been shifted by 0.025 in order to fit the system of dataset I. Figure 9 gives the shifted differential magnitudes from run 11 and some of the quasi simultaneous differential b magnitudes from run 10 as a function of time. From that Figure, one can conclude that the agreement is always perfect and that one can be confident of the data analyzed here.

Figure 9 can also illustrate the third point that justifies the existence of dataset III. Dataset III contains several measurements per night, in order to roughly investigate the problem of the one-day aliasing and of the related dubiousness about the high frequency variations. Inspection of Figure 9 suggests that the star varies within the night although the night-to-night variation is somewhat larger.

We have reported in Table X the nightly means and standard deviations as well as the corresponding night-to-night quantities. These values support the impression coming from Figure 9: the mean nightly variance is five times less than the night-to-night variance indicating that the low frequency variations have more power than the high frequency ones. Nevertheless, the nightly variance is larger than the observational errors proving that the star also varies on a short time scale of a few hours.

3.3 THE DATA ACQUIRED AT SAOO (DATASET IV). — Balona and Egan (1989) and Balona, Egan and Marang (1989a, b) have presented and analyzed an extensive photometric (Strömgren b) dataset for WR16. These observations were made using the Volks photometer attached at the 50cm telescope of the Sutherland site of the South African Astronomical Observatory. The comparison stars were HD88907 and HD89104. We will label these data, dataset IV. It is made of two almost continuous runs, one spans from JD2447173 to JD2447199, whereas the other is from JD2447230 to JD2447291. The natural width is of the order of 0.008 d^{-1}. The total number of measurements is 370 distributed over 57 nights, several of the nights having more than 10 measurements. Such a configuration is interesting in order to investigate the high frequency variations of the star. The mean nightly standard deviation for WR16 is about 0.005, slightly larger than 0.003, the corresponding quantity for the comparison stars. This confirms the slight variability of the star on short time scales. The night-to-night standard deviation for WR16 is found to be 0.016. Consequently, the night-to-night variance is 10 times larger than the nightly one, indicating well-marked low frequency variations of the Wolf-Rayet star.

TABLE X. — *Means (above) and standard deviations (below) of the differential magnitudes corresponding to each day of observation of run 11 (dataset III). We give also the night-to-night means and standard deviations as well as the total ones.*

HJD(2440000+)	V-(C_1+C_2)/2	C_1-C_2	C_1-C_3
7591.	0.2619	0.2090	−0.2929
	0.0031	0.0006	0.0011
7592.	0.2655	0.2092	−0.2934
	0.0015	0.0007	0.0008
7593.	0.2538	0.2098	−0.2931
	0.0025	0.0019	0.0019
7594.	0.2674	0.2085	−0.2941
	0.0047	0.0056	0.0022
7595.	0.2759	0.2087	−0.2924
	0.0052	0.0007	0.0006
7596.	0.2641	0.2109	−0.2931
	0.0052	0.0003	0.0015
7597.	0.2762	0.2095	−0.2941
	0.0037	0.0007	0.0004
7598.	0.2523	0.2082	−0.2918
	0.0035	0.0012	0.0010
Night-to-night	0.2646	0.2092	−0.2931
	0.0088	0.0009	0.0008
All	0.2645	0.2092	−0.2931
	0.0090	0.0019	0.0013

The present data have been analyzed using Fourier techniques. The two runs do not show the same mean magnitude as can be seen on Figure 3 of Balona, Egan and Marang (1989b). As a consequence, peaks of very low frequencies appear in the power spectrum. We think that this cannot be attributed to a variation of the star since, as pointed out in section 3.1.3, our data suggest it is very stable on a very long time baseline. This can be due to the inhomogeneous sampling. Whatsoever, in order to continue our analysis, we have been obliged to remove the first trend from the data. The power spectrum has been explored up to a few tens of d^{-1}. Clearly, all the power is located below $\nu \sim 1.5\,d^{-1}$. The lower part of the power spectrum is given in Figure 10: a peak is visible at $\nu_1 = 0.058\,d^{-1}$ ($P = 17.24$ d), in good agreement with the results of Balona, Egan and Marang (1989b). It corresponds to a semi-amplitude $a = 0.0130$ ($\sigma_a = 0.0011$), a normalized power of $P_N = 58.4$ and, of course, a significance level virtually equal to zero.

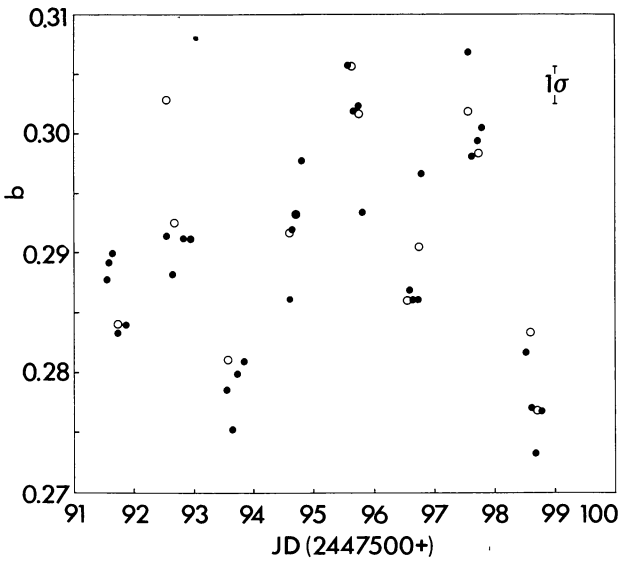

FIGURE 9. — Strömgren *b* filter differential magnitudes of dataset III (shifted by 0.025 mag., symbol •) and some contemporaneous measurements from run 10 (dataset I, symbol ○). The error bar represents one standard deviation of the measurements of dataset I as deduced from the comparison stars. The standard deviation corresponding to dataset III is about two thirds of that.

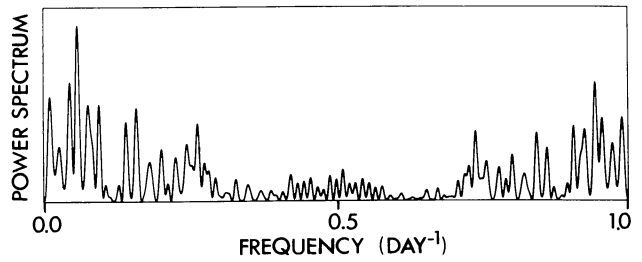

FIGURE 10. — Same as Figure 1 but corresponding to the differential magnitudes of dataset IV.

The semi-amplitude is of the same order but significantly larger than what we usually observe in dataset I. The large normalized power can be explained by the fact that we are testing the data against the null-hypothesis of white-noise. The hypothesis is of course rejected by the sole statement that the night-to-night variance is 10 times larger than the nightly one; this rejection induces the large value observed here. A more reasonable approach consists in reducing the data to one point per night. The normalized power is then $P_N = 7.1$ and turns out to be no more significant. Nevertheless, the data have been prewhitened for this frequency and analyzed again. No peak is clearly outstanding but we can spot one at $\nu = 0.011\ d^{-1}$ and another at $\nu = 0.158\ d^{-1}$; they are not significant.

As a conclusion, the dataset IV is not able by itself to demonstrate the existence of a significant periodicity. However, a typical frequency of $\nu = 0.058\ d^{-1}$ is suggested and a similar value was already noticed in an independent way in dataset I (it is only a natural width away from $\nu = 0.066\ d^{-1}$).

3.4 THE COMBINED DATASET I+II+III+IV. — The global dataset I+II+III+IV has been built up by combining all the *b* filter measurements. Dataset III has been shifted by 0.025 mag. in order to fit the system of dataset I. Run 9 which has been transformed to the 1m system has also been shifted by the same amount. A few points of run 6 are quasi contemporaneous (only a longitude effect) with observations of dataset IV. From this overlap, we deduce that dataset IV has to be shifted down by 1.806 mag.; the agreement between the two datasets is very good. The global dataset I+II+III+IV is constituted of 282 measurements and the variance is 1.7×10^{-4} square mag.; Figure 11 gives the power spectrum of the data: a peak is slightly dominating at $\nu_1 = 0.1098\ d^{-1}$ ($P = 9.107$ d). This peak corresponds to a semi-amplitude $a = 0.0062$ ($\sigma_a = 0.0010$) and to a normalized power of 16.1. The corresponding CSL is 0.0003. Although this frequency is significant, the semi-amplitude is still smaller than the relevant semi-amplitude observed for dataset I and, *a fortiori*, than the one of dataset Ia. The data have been prewhitened for this frequency and reanalyzed. The power spectrum is constituted of a forest of peaks between 0.0 d^{-1} and 0.25 d^{-1}, no further frequency could be spotted. The forest of peaks is already visible in Figure 11 as well as the lack of power between 0.25 d^{-1} and 0.50 d^{-1}. Consequently, the residual variability cannot be modelled or even approximated by a white-noise process.

It is interesting to remark that the different datasets seem each to induce a few peaks in the power spectrum but that no global coherency exists. This remark also holds for ν_1 whose semi-amplitude is particularly small and could almost be considered as a remaining of dataset Ia without large contribution from other datasets.

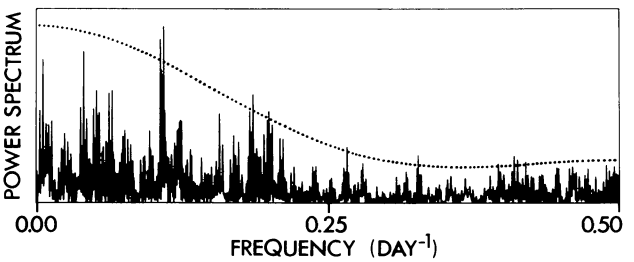

FIGURE 11. — Same as Figure 1 but corresponding to the differential magnitudes of the global dataset I+II+III+IV. See section 5.2 for an explanation of the dotted line.

4. Analysis of the polarimetric data.

In 1986, polarimetric data during a continuous 42 night run, have been acquired by Drissen *et al.* (1987). They suggest

the existence of a mildly preferred axis for the polarization but conclude that any systematic effect seems to be masked by stochastic variability. Figure 12 gives the power spectrum of the polarization amplitude. Two peaks are clearly visible, one at $\nu_1 = 0.220\,\mathrm{d}^{-1}$ ($P = 4.545$ d) and the other at $\nu_2 = 0.063\,\mathrm{d}^{-1}$ ($P = 15.87$ d); both exist independently of each other. These deviations from randomness are not significant by themselves as already pointed out by Drissen *et al.* (1987) and as confirmed by our computation of the CSL and the NSL. However, the natural width of this dataset being $0.024\,\mathrm{d}^{-1}$, we can say that, astonishingly, the present frequency ν_2 is quite compatible with ν_2 of dataset I and the present frequency labelled ν_1 is only slightly different from the one named ν_3 in the case of dataset I. The analysis of the time variations of the angle θ of the polarization leads to a flat power spectrum permitting no further conclusions.

A few points from run 2 and run 3 are quasi simultaneous with the polarimetric observations. The datasets have been cross-correlated using the method of Edelson and Krolik (1988). No clear relation between the photometry and the polarimetry has been found beyond the fact that the marked light minimum around JD2446518 corresponds to a relative decrease of the polarization by 10% ($\sim 3\sigma$ effect).

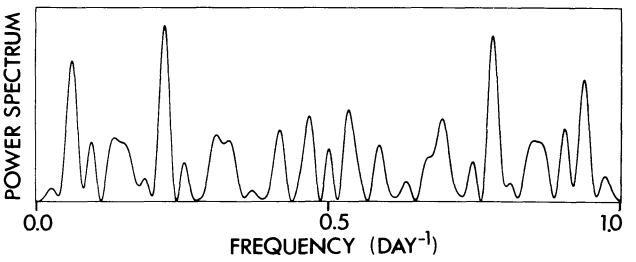

FIGURE 12. — Power spectrum (method of Deeming, 1975) of the polarization amplitude of WR16. The ordinates are in arbitrary units.

5. Discussion and further results.

5.1 THE VARIABILITY OF WR16 AS A DETERMINISTIC PROCESS. — Analysis of the data presented here suggests the existence in WR16 of a periodicity with $\nu_A \sim 0.110\,\mathrm{d}^{-1}$ ($P_A = 9.100$ d). This was already reported by Lamontagne and Moffat (1987; with variable comparison stars) and by van Genderen, van der Hucht and Bakker (1989) (on the basis of runs 1, 2, 3, 4). The latter qualified the variability as quasi-periodicity, a conclusion based on the general appearance of the lightcurve. We would like to insist here on the importance of discriminating between a true periodicity and a quasi-periodicity. The quasi-periodicity can be thought of as, for example, a phenomenon almost periodic but whose frequency and phase are to some extent subject to apparently random variations. However, a strictly periodic process, if immersed in a stochastic process (noise or random variability), can generate lightcurves that, at first sight, have the same characteristics. It is of the highest importance to distinguish between the two because they have fundamentally different implications about the nature of the star. We would like to introduce now a way to address the question. The method we will employ was first suggested by Eddington and Plakidis (1929) and has been recently brought into use again by Blacher and Perdang (1988). We list below the times of the marked minima relevant to P_A. We give an ordinal number and the heliocentric julian date (HJD-2440000)

1	6415.716,
2	6427.835,
3	6437.838,
8	6482.708,
9	6491.312,
10	6502.716,
11	6513.682.

The difference of two consecutive minima is an estimation of the period. We have at our disposal five such differences, leading to a mean of $\mu_1 = \bar{P} = 10.62$ d and a standard deviation $\sigma_1 = 1.36$ d. We can also consider the differences between the first and the third minima, the eighth and the tenth ones, and the ninth and the eleventh ones. These second order differences lead to $\mu_2 = 21.50$ d ($\bar{P} = 10.75$ d) and to $\sigma_2 = 1.30$ d. Finally, the three seventh order differences lead to $\mu_7 = 65.12$ d ($\bar{P} = 9.43$ d) and $\sigma_7 = 1.77$ d. The main point is that, in the case of a periodic signal hidden in the "noise", the σ_i should be constant. On the opposite, for random and chaotic processes, the σ_i should increase with i (Blacher and Perdang, 1988). The increase is proportional to i for completely random processes. In our case, σ_7 is not significantly different from σ_1 or σ_2. Of course, we are dealing here with small number statistics. We thus conclude that, at least, the existing data do not permit to conclude to the existence of a quasi-periodicity rather than of a periodicity. In addition, the data are rather suggestive of a periodicity hidden in the noise, but due to the small number of reported minima, edge effects could be expected (i.e. the population of minima used is dependent on the order of the difference). The value of σ_8 is also very small, confirming our conclusions based on σ_7.

If we admit the existence of ν_A, we are constrained to accept that a second periodicity $\nu_B = 0.066\,\mathrm{d}^{-1}$ ($P_B = 15.15$ d) is also present (supported by dataset Ia, I and perhaps also dataset IV and the polarimetric data). In addition, we cannot neglect the most probable existence of a third periodicity $\nu_C = 0.183\,\mathrm{d}^{-1}$ ($P_C = 5.464$ d). They are all three significant (and particularly the first two) against a white-noise null-hypothesis. Once the three frequencies are removed from the data, it turns out that the star is also varying in a random way with a variance of about $1\text{-}1.5 \times 10^{-4}$ square mag. The latter process is very near white-noise. The data we have now at hand are, unfortunately, still

not numerous enough to study the consistency of the three frequencies simultaneously. We mean that it is not possible to state either that we are dealing with pseudo-periodicities occuring from time to time and only surviving a few cycles (some ten cycles for ν_A, the only "visible" one) or that we have to deal with physical periodicities sometimes hidden in the stochastic process.

However, when all the reliable data are gathered together and analyzed, only ν_A can still be suspected to be present and the power spectrum of Figure 11 exhibits essentially a forest of peaks between 0.0 d^{-1} and 0.25 d^{-1}. This behaviour is more reminiscent of a stochastic process and the lack of power beyond $\nu = 0.25\ d^{-1}$ is suggestive of a correlated random process. We will address this possibility in the following section.

5.2 THE VARIABILITY OF WR16 AS A STOCHASTIC PROCESS. — Usually, the study of the variability of Wolf-Rayet stars is confined to the search for periodicities -i.e. for deterministic processes- and are limited to frequency domain analyses. We would like to take the opportunity of our remarks at the end of section 5.1 to try to make a first, small step towards time domain analysis and stochastic processes.

The Wold theorem (Wold, 1938) establishes that any stationary process, with its purely deterministic part removed, can be represented as a Moving Average (MA) process, as an Auto-Regressive (AR) process or as a mixed Auto-Regressive Moving Average (ARMA) process (Scargle, 1981). If we admit that no deterministic part is present in dataset I+II+III+IV, we can try to represent the variability of WR16 following one of these possibilities. An MA representation of a process can be expressed as the convolution of a white-noise process **R** by a filter **C** containing most or all the deterministic aspect (e.g. correlations) of the random process. The vector of the modified observations **X** is therefore given by the convolution

$$\mathbf{X} = \mathbf{R} * \mathbf{C}.$$

As pointed out by Scargle (1981), the MA model expresses the correlations in a process in terms of memory or remanence. On the other hand, an AR model expresses them by remembering its own behaviour at previous time. The instantaneous importance of each of its behaviours can be included in a vector **A** and we have the following expression

$$\mathbf{R} = \mathbf{A} * \mathbf{X}.$$

In most of the cases, both MA and AR, as well as their mixing ARMA, are strictly equivalent mathematical representations. Therefore, the choice (identification) is usually based on the notion of parsimony that consists in selecting the model with the smallest number of parameters. This choice is not to be considered as absolutely valid but it is an attempt to find a simple, physically suggestive model. In addition, it can always be considered as a first approximation to be improved later. The advantage of these methods is to separate the deterministic part of the random process (**C** or **A**) from the white-noise process **R**, also called the innovation, that should contain the stochastic aspect of the process.

The first step of the analysis is to compute the autocorrelation function of dataset I+II+III+IV. The relative scarcity of the present data and the great unevenness of the sampling preclude a sophisticated deconvolution of the data: consequently, we are constrained to work not on the data themselves but on the autocorrelation function.

The computational method of Edelson and Krolik (1988) has been used to calculate the autocorrelation function of dataset I+II+III+IV that is given in Figure 13. We can see that the correlation virtually vanishes beyond a time lag of about two days. Such a vanishing autocorrelation is typical of a finite MA process. As we are constrained to limit our investigation to the autocorrelation function, an ambiguity appears in the sense that the deconvolution of $\mathbf{R} * \mathbf{C}$ is not unique. A family of filters **C** gives rise to the same autocorrelation function. However, we rely on Wold's (1938) approach and select the causal, minimum delay, member of the family (see Scargle, 1981). Let us render the process discrete with a step of one day (the natural low frequency sampling interval). From Figure 13, we can deduce that the MA process is of order 2 as only the first two points of the autocorrelation are markedly different from zero. We read the correlations at lag one and at lag two as being, respectively,

$$\rho 1 = 0.40$$
$$\rho 2 = 0.15.$$

From Box and Jenkins (1976), we know that the ρi can be related to the filter components C_i by

$$\rho 1 = \frac{C_1 (1 + C_2)}{1 + C_1^2 + C_2^2}$$
$$\rho 2 = \frac{C_2}{1 + C_1^2 + C_2^2}.$$

We deduced $C_1 = 0.40$ and $C_2 = 0.18$ and the process can be represented by

$$X_n = R_n + 0.40\, R_{n-1} + 0.18\, R_{n-2}.$$

As the variance of the observations is about 1.7×10^{-4} square mag., we can deduce a variance

$$\sigma_R^2 = \frac{1.7 \times 10^{-4}}{1 + C_1^2 + C_2^2} = 1.4 \times 10^{-4}$$

for the innovation **R**. The power at frequency ν of such an MA process is given, within a factor, by $P(\nu) \propto (1 + C_1^2 + C_2^2 + 2C_1 (1 + C_2) \cos (2\pi\nu) + 2C_2 \cos 4\pi\nu)$.

This continuous spectrum is shown in Figure 11 as a dotted line. Clearly, it envelops very well the observed spectrum confirming that the MA process of order two is not a bad approximation of the observed variability corresponding to dataset I+II+III+IV.

Because we cannot safely apply deconvolution methods (such as the one suggested by Scargle, 1981, or by Scargle, 1989) to the data, we are not able to deduce the innovation corresponding to our observations. This prevents us from deciding what is the exact type of the apparently random component of the variability of WR16. Effectively, the knowledge of the innovation permits to decide whether we have to deal with a usual, pure, true MA process or with a chaotic MA process (see Scargle, 1989) or with a mixing of both. The innovation of an MA process is a white-noise process whereas the innovation relevant to a chaotic process as viewed by Scargle (1989) exhibits a somewhat deterministic behaviour.

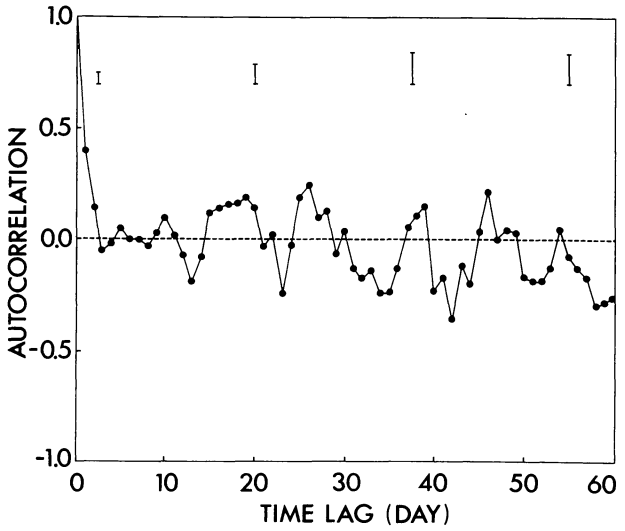

FIGURE 13. — Autocorrelation function of the Strömgren *b* filter differential magnitudes of the global dataset I+II+III+IV given against the characteristic time lag. For the sake of clarity, only a few error bars are given. They represent one standard deviation.

Although we have shown that the general characteristics of dataset I+II+III+IV are quite compatible with an MA process, some question marks persist before we can identify the variability of WR16 with such a process. The main problem is that we have to explain the presence of the peak at ν_A in the power spectrum of dataset I+II+III+IV but also of the peaks at ν_A, ν_B and ν_C in the power spectra of dataset I or of dataset Ia. These peaks are significant against the null-hypothesis of white-noise. The question is: are they abnormal for an MA process?

Therefore, we adopt here as a null-hypothesis, the MA process of order two described above. We have gathered several realizations of such a process, and for each of them we have spotted the highest peak in the power spectrum and have kept its power in memory. As above, these simulations permit us to test the null-hypothesis and to derive a corresponding CSL. Immediately, it becomes evident that the normalized power could reach, between $\nu = 0.0\,d^{-1}$ and $\nu \sim 0.5\,d^{-1}$ (particularly below $\nu = 0.25\,d^{-1}$), very high values, some realizations exhibiting values greater than 20. Concerning the dataset Ia, the normalized power of 16.5 observed for the *b* filter magnitudes is attained once is twenty five trials if we inspect all the frequency domain, whereas it is attained once in fifty trials if we consider frequencies between $\nu = 0.09\,d^{-1}$ and $\nu = 0.25\,d^{-1}$. The corresponding CSL is thus between 0.02 and 0.04. The CSL's for the other spotted frequencies and for the other filters are markedly larger. Concerning dataset I, all the normalized powers given in Table IX are easily reached leading to large CSL's and thus to no significant deviation from the null-hypothesis. The situation is similar with respect to the existence of ν_A in dataset I+II+III+IV. Therefore, we conclude that no observed normalized power is too large with respect to the expectation under the null-hypothesis of the adopted MA(2) process.

These results concern the power of the highest peak in the power spectrum. The spectrum given in Figure 1 is strongly reminiscent of the power spectrum of a single periodicity and one could worry about the compatibility of the null-hypothesis with such isolated peaks. We have visually inspected some of the power spectra of the simulated data and we arrived at the conclusion that, at least, one spectrum in one hundred exhibits an isolated peak like the one of Figure 1.

Because of the stochastic nature of the model, a direct comparison between the observed lightcurve and the synthetic one is not possible. In addition, the display of one of the realizations would not help in illustrating our conclusions.

6. The stability of the comparison stars.

In order to secure our results, we need a detailed investigation of the stability of the comparison stars. From an inspection of Table VI, where the standard deviations corresponding to the differential magnitudes C_1-C_2 relevant to each of the four filters and to dataset I are given, we can conclude that the observed dispersion is of the order of the expected error of the present differential photometry. As a further check, we computed the power spectra of the data. For each of the four filters, the power spectra of the data relevant to dataset Ib and dataset I are in good agreement with white-noise and no problem is to be pointed out. However, concerning dataset Ia, it is immediately clear that some anomaly exists. The power spectrum of the differential magnitudes C_1-C_2 relevant to dataset Ia is given in Figure 14 for each filter. The latter figure suggests the existence of two periodicities at $\nu_\alpha = 0.273\,d^{-1}$ (or the alias $0.727\,d^{-1}$) and $\nu_\beta = 0.376\,d^{-1}$ (or the alias $0.625\,d^{-1}$). The deviation from the null-

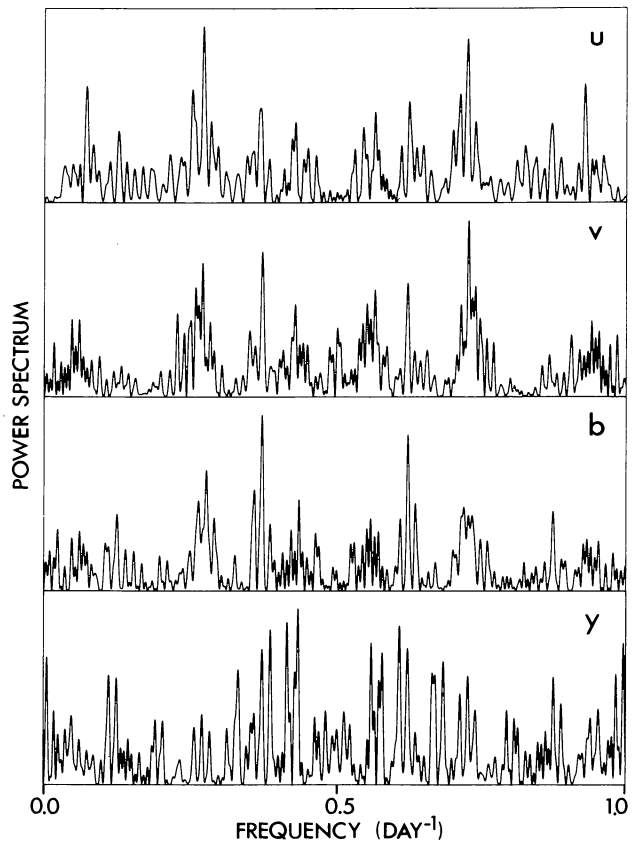

FIGURE 14. — Same as Figure 1 but corresponding to the differential magnitudes between the two comparison stars of dataset Ia ($C_1 - C_2$). Each panel corresponds to a different filter.

hypothesis of white-noise is never markedly significant; nevertheless, the effect leaps to the eyes. The relevant semi-amplitudes are also extremely low (of the order of 0.0015 mag.). The given frequencies are tentative because of the $\Delta\nu \sim 0.013\,d^{-1}$ aliasing present in the data and of the low level of the signal. In any case, we think it safer to limit us, as we did in our investigation of WR16, to resulting semi-amplitudes of about 0.006 mag. because the possible variability of the comparison stars could interact with the variability of the Wolf-Rayet in an indirect way. It is interesting to point out that ν_α is more marked in the blue-violet region (u, v filters) whereas, on the opposite, ν_β is preferentially present in the visible (b, y filters).

During run 11, we added a third comparison star in order to find which of C_1 or C_2 was responsible for the observed anomaly. Unfortunately, as can be deduced from Table X, we failed in our task. Evidently, all three stars were rather constant during that run and none of the two frequencies was present. This supports the idea that the relevant amplitudes are highly variable as neither dataset II or III nor dataset Ib exhibits the effect. The ambiguity can be removed by analyzing the absolute magnitudes of C_1 and C_2 separately. But the relevant power spectra are dominated by peaks induced by the observational effects and the phenomenon we are looking for is drowned in a forest of peaks. Nevertheless, comparatively to the power spectra relevant to C_2, the power spectra relevant to C_1 certainly exhibit more power at ν_α and its aliases and also, but to a fewer extent, at ν_β and its aliases. Thus, we think it safe to tentatively attribute both possible frequencies to C_1, i.e. HD86000.

Finally, we recall that Manfroid, Gosset and Vreux (1987) found from their differential photometry WR16/HD86000, two frequencies, namely $\nu = 0.74\,d^{-1}$ (or its alias 0.27 d^{-1}) and $\nu = 0.39\,d^{-1}$ (or its alias 0.61 d^{-1}). The relevant semi-amplitudes were about 0.01 mag. in the Strömgren b filter. Manfroid, Gosset and Vreux (1987) also reported the presence of $\nu = 0.57\,d^{-1}$ (or its alias 0.43 d^{-1}) and of $\nu = 0.75\,d^{-1}$ in the Walraven differential photometry WR16/HD86000 of van Genderen, van der Hucht and Steemers (1987), although total confidence cannot be attributed to the conclusions based on such a small amount of data. All these frequencies are quite compatible with ν_α and ν_β, and we therefore suggest that HD86000 is indeed variable with these two frequencies but that the amplitudes are extremely time varying. One could object that these frequencies seem to be absent from the differential magnitudes HD86199–HD86000 of Manfroid, Gosset and Vreux (1987). A reanalysis of these data suggests that ν_β is present but the time basis is too short and ν_β is blended with the harmonic of $\nu = 0.182\,d^{-1}$. If ν_β is actually present in HD86000, the coefficients A_2 and Φ_2 corresponding to the Ap star in Manfroid, Gosset and Vreux (1987) can thus be highly vitiated. On the other hand, the same reanalysis does not permit us to attribute ν_α to HD86000 rather than to the Wolf-Rayet star: the variability of WR16 is such that an ambiguity persists. As a conclusion, we suggest that HD86000 is probably responsible for part of the variability observed in the differential photometry of Manfroid, Gosset and Vreux (1987). The differential magnitudes $C_1 - C_2$ corresponding to dataset I are given in Table XI.

TABLE XI. — *Differential magnitudes C_1-C_2 corresponding to dataset I as a function of the heliocentric julian date of observation and of the Strömgren filter utilized.*

HJD(2440000+)	u	v	b	y
6412.8208	0.3704	0.2537	0.2078	0.1863
6413.7954	0.3786	0.2586	0.2154	0.1904
6414.7939	0.3748	0.2544	0.2120	0.1855
6415.7161	0.3733	0.2478	0.2102	0.1900
6415.8191	0.3781	0.2552	0.2120	0.1866
6416.7359	0.3726	0.2561	0.2144	0.1850
6416.8154	0.3733	0.2513	0.2086	0.1861
6420.8050	0.3636	0.2510	0.2045	0.1849
6421.7512	0.3724	0.2532	0.2074	0.1825
6421.8205	0.3749	0.2600	0.2151	0.1889
6422.7368	0.3771	0.2577	0.2103	0.1875
6422.8175	0.3747	0.2549	0.2160	0.1867
6423.7202	0.3677	0.2491	0.2063	0.1846
6423.8292	0.3674	0.2546	0.2109	0.1861
6424.7097	0.3778	0.2556	0.2133	0.1932
6424.8229	0.3685	0.2514	0.2096	0.1829
6425.7234	0.3791	0.2598	0.2155	0.1858
6425.8335	0.3792	0.2599	0.2175	0.1911
6427.7256	0.3763	0.2632	0.2122	0.1906
.6427.8348	0.3747	0.2514	0.2118	0.1875
6428.7029	0.3679	0.2565	0.2083	0.1907
6428.8372	0.3763	0.2561	0.2171	0.1862
6429.7074	0.3876	0.2633	0.2199	0.1893
6429.8356	0.3766	0.2596	0.2145	0.1882
6430.7108	0.3715	0.2545	0.2129	0.1841
6430.8337	0.3768	0.2573	0.2133	0.1849
6431.6972	0.3648	0.2528	0.2070	0.1851
6431.8470	0.3655	0.2524	0.2101	0.1870
6432.6868	0.3780	0.2533	0.2110	0.1906
6432.8468	0.3839	0.2589	0.2168	0.1848
6433.6851	0.3731	0.2566	0.2129	0.1910
6433.8428	0.3755	0.2581	0.2151	0.1888
6434.6873	0.3698	0.2528	0.2089	0.1858
6434.8402	0.3684	0.2565	0.2148	0.1941
6435.6783	0.3751	0.2532	0.2108	0.1871
6435.8394	0.3667	0.2516	0.2124	0.1884
6436.6773	0.3775	0.2582	0.2153	0.1926
6436.8392	0.3809	0.2557	0.2142	0.1839
6437.6849	0.3709	0.2475	0.2068	0.1844
6437.8380	0.3769	0.2552	0.2122	0.1883
6439.6897	0.3660	0.2571	0.2108	0.1926
6439.8422	0.3721	0.2547	0.2092	0.1807
6440.6795	0.3637	0.2551	0.2092	0.1920
6440.8421	0.3726	0.2561	0.2158	0.1906
6441.6824	0.3775	0.2585	0.2151	0.1904
6441.8455	0.3760	0.2578	0.2130	0.1873
6442.6835	0.3800	0.2531	0.2129	0.1845
6442.8376	0.3686	0.2515	0.2115	0.1839
6443.6800	0.3755	0.2587	0.2195	0.1953
6443.8279	0.3866	0.2643	0.2216	0.1920
6476.7154	0.3781	0.2532	0.2117	0.1844
6477.8182	0.3684	0.2567	0.2140	0.1911
6478.7287	0.3709	0.2574	0.2102	0.1836
6479.8451	0.3741	0.2522	0.2123	0.1929
6480.6131	0.3781	0.2551	0.2142	0.1878
6480.7846	0.3750	0.2560	0.2099	0.1846
6481.6637	0.3824	0.2577	0.2147	0.1889
6481.7999	0.3683	0.2540	0.2118	0.1921
6482.7076	0.3671	0.2533	0.2119	0.1915
6483.7649	0.3817	0.2570	0.2155	0.1903
6484.7593	0.3780	0.2556	0.2105	0.1850
6486.6889	0.3738	0.2552	0.2137	0.1907
6487.7463	0.3776	0.2534	0.2105	0.1893
6488.7345	0.3742	0.2543	0.2134	0.1917
6489.7209	0.3765	0.2569	0.2170	0.1915
6490.7501	0.3730	0.2538	0.2127	0.1847
6491.6722	0.3688	0.2566	0.2158	0.1985
6491.7976	0.3730	0.2553	0.2097	0.1862
6492.6984	0.3747	0.2582	0.2109	0.1886
6493.7434	0.3697	0.2513	0.2090	0.1843
6493.8198	0.3646	0.2560	0.2151	0.1897
6494.7045	0.3697	0.2587	0.2126	0.1902
6495.7134	0.3685	0.2552	0.2047	0.1857
6496.6526	0.3721	0.2559	0.2113	0.1864
6496.8129	0.3775	0.2560	0.2114	0.1876
6498.6538	0.3787	0.2551	0.2107	0.1870
6499.7489	0.3790	0.2533	0.2143	0.1872
6500.6820	0.3735	0.2551	0.2119	0.1877
6501.7022	0.3755	0.2562	0.2102	0.1845
6502.7141	0.3776	0.2589	0.2130	0.1898
6503.5870	0.3761	0.2568	0.2104	0.1911
6503.7182	0.3650	0.2527	0.2059	0.1843
6504.7035	0.3678	0.2605	0.2148	0.1938
6504.7721	0.3738	0.2582	0.2112	0.1844
6505.7256	0.3771	0.2556	0.2130	0.1906
6505.7771	0.3739	0.2541	0.2096	0.1887
6506.6069	0.3712	0.2558	0.2082	0.1908
6506.7870	0.3771	0.2548	0.2128	0.1896
6507.5516	0.3705	0.2531	0.2114	0.1931
6507.7557	0.3837	0.2568	0.2170	0.1931
6508.7185	0.3752	0.2555	0.2117	0.1888
6509.6554	0.3779	0.2605	0.2168	0.1925
6509.7475	0.3703	0.2534	0.2076	0.1862
6510.6758	0.3773	0.2582	0.2119	0.1929
6511.6484	0.3768	0.2520	0.2110	0.1808
6512.6704	0.3793	0.2584	0.2107	0.1910
6513.6823	0.3814	0.2583	0.2161	0.1888
6516.7031	0.3720	0.2536	0.2087	0.1890
6517.6755	0.3661	0.2576	0.2117	0.1910
6518.6018	0.3697	0.2572	0.2113	0.1896
6518.7570	0.3698	0.2542	0.2113	0.1892
6519.6462	0.3697	0.2499	0.2111	0.1894
6519.7687	0.3761	0.2564	0.2122	0.1839
6581.4878	0.3693	0.2498	0.2060	0.1832
6582.4910	0.3748	0.2548	0.2110	0.1857
6583.5150	0.3700	0.2531	0.2078	0.1847
6584.4771	0.3739	0.2549	0.2151	0.1911
6585.4718	0.3718	0.2514	0.2097	0.1864

TABLE XI (*continued*)

HJD(2440000+)	*u*	*v*	*b*	*y*
6587.4823	0.3737	0.2550	0.2117	0.1892
6588.5082	0.3708	0.2538	0.2093	0.1841
6589.4788	0.3736	0.2549	0.2143	0.1901
7147.8380	0.3721	0.2550	0.2125	0.1838
7148.8301	0.3687	0.2533	0.2100	0.1863
7150.8406	0.3778	0.2507	0.2115	0.1855
7151.8323	0.3784	0.2599	0.2146	0.1895
7152.8217	0.3730	0.2552	0.2124	0.1879
7155.7982	0.3714	0.2542	0.2086	0.1838
7156.8286	0.3618	0.2505	0.2076	0.1831
7158.8039	0.3721	0.2563	0.2121	0.1880
7159.7710	0.3661	0.2548	0.2083	0.1867
7160.7636	0.3739	0.2539	0.2111	0.1872
7161.8173	0.3803	0.2568	0.2139	0.1853
7162.8080	0.3735	0.2525	0.2091	0.1837
7164.7651	0.3709	0.2560	0.2106	0.1860
7165.7374	0.3771	0.2508	0.2101	0.1865
7166.6958	0.3776	0.2567	0.2115	0.1868
7167.7432	0.3769	0.2538	0.2108	0.1814
7167.8062	0.3690	0.2542	0.2102	0.1885
7168.6749	0.3697	0.2506	0.2074	0.1837
7168.8058	0.3732	0.2548	0.2088	0.1855
7169.6851	0.3731	0.2536	0.2108	0.1877
7169.7997	0.3737	0.2556	0.2103	0.1826
7170.7017	0.3765	0.2618	0.2158	0.1945
7171.7370	0.3762	0.2516	0.2105	0.1873
7171.8309	0.3755	0.2525	0.2115	0.1855
7172.7390	0.3792	0.2598	0.2138	0.1894
7172.8191	0.3836	0.2629	0.2215	0.2030
7173.7439	0.3742	0.2581	0.2144	0.1900
7173.8191	0.3676	0.2549	0.2110	0.1885
7174.7224	0.3696	0.2567	0.2109	0.1884
7174.8425	0.3778	0.2571	0.2125	0.1859
7175.7324	0.3746	0.2553	0.2089	0.1843
7175.8457	0.3689	0.2532	0.2098	0.1875
7176.7418	0.3671	0.2542	0.2095	0.1849
7176.8507	0.3720	0.2557	0.2112	0.1845
7177.7372	0.3739	0.2543	0.2094	0.1882
7177.8487	0.3774	0.2590	0.2137	0.1875
7178.7363	0.3697	0.2515	0.2078	0.1860
7178.8545	0.3671	0.2518	0.2080	0.1885
7179.7351	0.3760	0.2551	0.2135	0.1854
7179.8494	0.3705	0.2540	0.2107	0.1863
7180.7289	0.3708	0.2561	0.2121	0.1899
7180.8536	0.3764	0.2589	0.2138	0.1903
7475.8291	0.3763	0.2592	0.2203	0.1911
7476.7995	0.3809	0.2647	0.2170	0.1901
7477.8065	0.3679	0.2555	0.2108	0.1823
7478.7900	0.3834	0.2537	0.2094	0.1850
7479.7780	0.3769	0.2526	0.2089	0.1884
7480.7848	0.3667	0.2537	0.2084	0.1898
7481.7767	0.3695	0.2518	0.2071	0.1775
7482.7779	0.3687	0.2567	0.2153	0.1946
7483.8348	0.3657	0.2563	0.2045	0.1914
7484.7779	0.3673	0.2530	0.2115	0.1927
7486.7766	0.3833	0.2630	0.2179	0.1941
7487.7879	0.3654	0.2596	0.2140	0.1851
7488.7604	0.3677	0.2510	0.2059	0.1937
7489.7637	0.3673	0.2486	0.2066	0.1871
7490.7602	0.3820	0.2533	0.2075	0.1885
7491.7459	0.3798	0.2606	0.2155	0.1819
7492.7519	0.3685	0.2528	0.2160	0.1967
7493.7451	0.3728	0.2544	0.2107	0.1901
7494.7633	0.3677	0.2568	0.2080	0.1966
7495.7444	0.3818	0.2513	0.2059	0.1713
7590.7581	0.3734	0.2552	0.2120	0.1907
7591.7319	0.3774	0.2543	0.2133	0.1900
7592.5654	0.3689	0.2524	0.2104	0.1873
7592.6599	0.3726	0.2536	0.2087	0.1893
7593.5519	0.3679	0.2540	0.2089	0.1824
7594.5829	0.3752	0.2548	0.2092	0.1849
7594.6927	0.3739	0.2585	0.2150	0.1918
7595.6085	0.3734	0.2532	0.2129	0.1825
7595.7213	0.3718	0.2525	0.2110	0.1862
7596.5605	0.3709	0.2548	0.2087	0.1883
7596.7287	0.3702	0.2548	0.2101	0.1873
7597.5480	0.3665	0.2483	0.2058	0.1838
7597.7108	0.3816	0.2526	0.2120	0.1871
7598.6104	0.3717	0.2513	0.2088	0.1838
7598.7162	0.3715	0.2496	0.2089	0.1845
7599.5836	0.3705	0.2549	0.2064	0.1876
7599.7312	0.3707	0.2578	0.2122	0.1893
7600.5542	0.3783	0.2629	0.2143	0.1904
7600.7845	0.3693	0.2571	0.2100	0.1879
7601.5999	0.3651	0.2518	0.2077	0.1851
7601.7136	0.3724	0.2474	0.2043	0.1805
7602.5330	0.3836	0.2657	0.2195	0.1944
7602.6973	0.3709	0.2540	0.2099	0.1867
7603.5754	0.3752	0.2565	0.2113	0.1882
7603.7495	0.3746	0.2546	0.2088	0.1843
7605.6267	0.3661	0.2534	0.2070	0.1869
7605.7439	0.3756	0.2587	0.2130	0.1873
7606.5794	0.3719	0.2645	0.2181	0.1895
7606.7438	0.3725	0.2554	0.2109	0.1872
7607.5665	0.3769	0.2568	0.2152	0.1944
7607.7272	0.3726	0.2576	0.2125	0.1919
7608.5857	0.3684	0.2511	0.2097	0.1860
7608.7146	0.3767	0.2545	0.2136	0.1892
7609.5580	0.3661	0.2553	0.2101	0.1859
7610.5775	0.3703	0.2548	0.2101	0.1891
7610.6924	0.3700	0.2556	0.2091	0.1835
7611.5536	0.3764	0.2554	0.2146	0.1871

HJD(2440000+)	u	v	b	y
7611.6947	0.3757	0.2507	0.2115	0.1876
7612.5935	0.3723	0.2522	0.2101	0.1859
7612.7220	0.3728	0.2555	0.2130	0.1910
7613.5574	0.3691	0.2496	0.2081	0.1830
7613.7068	0.3683	0.2510	0.2098	0.1878
7614.5689	0.3795	0.2585	0.2153	0.1892
7614.7451	0.3964	0.2679	0.2241	0.1956
7615.5920	0.3712	0.2556	0.2136	0.1863
7615.7190	0.3698	0.2560	0.2120	0.1849
7616.5548	0.3789	0.2553	0.2115	0.1842
7616.7205	0.3623	0.2514	0.2082	0.1878

7. Conclusion.

We have presented various new datasets of Strömgren differential photometry of the Wolf-Rayet star WR16. Our analysis of the latter, along with the study of previously published data, permits us to improve our ideas about the variability of that star. The precision of the photometry analyzed in the present paper, as deduced from the comparison stars, leads to a standard deviation of $\sigma \sim 0.003$ mag. The corresponding nightly dispersion of the WR16 measurements is $\sigma \sim 0.005$ mag. whereas the night-to-night dispersion gives rather $\sigma \sim 0.010 - 0.015$ mag. Therefore, the main part of the variability has essentially a low frequency nature. The variations are positively correlated on time lags up to about two days, a characteristic delay larger than the time of replacement of a typical Wolf-Rayet star wind. A detailed analysis shows that two frequencies $\nu_A = 0.110\,d^{-1}$ ($P_A = 9.100$ d) and $\nu_B = 0.066\,d^{-1}$ ($P_B = 15.15$ d) are present in the data and that a third one, $\nu_C = 0.183\,d^{-1}$ ($P_C = 5.464$ d) is most probably present. However, these frequencies are not present in all the datasets with the same powers and/or semi-amplitudes. Besides these three frequencies, a fourth component of the variability is present under the form of a random variation with a standard deviation of about 0.009-0.013 mag. The latter process is very near white-noise as long as frequencies lower than one d^{-1} are concerned. This random variation is clearly attributable to the Wolf-Rayet star. Its rather high power implies the difficulty we could have to discern periodicities and /or quasi-periodicities superimposed to it.

In addition, we have no reason to believe that the decomposition into four components of the variability seen in our data, is representative of the nature of WR16. In particular, the present data do not permit the testing of all the three frequencies for consistency at the same time. This, linked to the observed lack of stability for their semi-amplitudes and to the rather high number (three) of frequencies needed, has led us to investigate the alternative possibility that the three frequencies are only transient phenomena and that they are part of the same mechanism as the random variations. In this framework, we have shown that the low frequency variability of WR16 is well modelled by a Moving Average process of order two (with one-day steps). Such a process explains very well all the components of the arbitrary decomposition: the power of the frequencies ν_B and ν_C as well as the random variations. It could also explain the power of ν_A as, at the worst, one time in fifty, the power associated with ν_A in a particular dataset is smaller than the statistical prediction of the MA process.

It is the first time that attempts are made to model the variability of a Wolf-Rayet star by a stochastic process. The MA process described in this paper is able to explain all the presently known characteristics of the light variations of WR16 but should be considered as a first draft of a process to be refined later. Only future observations will put more severe constraints on our ideas about the variability of WR16. In particular, should a periodicity or a quasi-periodicity around ν_A be frequently observed again, it would imply the actual existence of ν_A. Such an observation would not necessarily reject the MA process model because ν_B, ν_C and perhaps other new frequencies would remain to be explained. The MA process would then cohabit with ν_A. Nevertheless, for the time being, the MA process has the advantage of the simplicity over the three or four component model.

Our data also suggest the possible (marginal) existence of very small amplitude light variations of the comparison star HD86000 with two characteristic frequencies ($\nu_\alpha = 0.273\,d^{-1}$ and $\nu_\beta = 0.376\,d^{-1}$ or their one-day aliases). The associated amplitudes are in fact time varying. It is necessary to mention that these two frequencies are virtually identical to the ones detected by Manfroid, Gosset and Vreux (1987) in their differential photometry WR16/HD86000 and that they tentatively attributed to WR16. Consequently, this attribution seems now doubtful (or even unlikely) and the relevant biperiodicity is most probably linked to HD86000.

Acknowledgments.

Part of the data were obtained, in the framework of the Long-term Photometry of Variables project at ESO, by E. Bibo, F.-J. Zickgraf, M. Burger, A. Jorissen, H. Steenman, Y.K. Ng, and M. Hiesgen. We are greatly indebted to all of them for their most important observational contribution. A lot of comments from L. Lucy have been determining and we want to express our thanks to him. This work has been partly supported by the Belgian Fund for Scientific Research through FNRS research grants to JMV and JM as well as through an NFWO research grant to CS.

References

ANDERSEN J., CLAUSEN J.V., NORDSTRÖM B., REIPURTH Bo: 1983, *Astron. Astrophys.* **121**, 271.

BALONA L.A., EGAN J.: 1989, in Physics of Luminous Blue Variables, *IAU colloquium* Nr. **113**, K. Davidson, A.F.J. Moffat, and H.J.G.L.M. Lamers, Eds. (Dordrecht: Kluwer Acad. Publ.), p. 307.

BALONA L.A., EGAN J., MARANG F.: 1989a, *South African Astron. Obs. Circ.* **13**, 55.

BALONA L.A., EGAN J., MARANG F.: 1989b, *Mon. Not. R. Astron. Soc.* **240**, 103.

BLACHER S., PERDANG J.: 1988, in Multimode Stellar Pulsations, proc. of a workshop held in Budapest, Hungary, 1-3 September 1987, G. Kovács, L. Szabados, and B. Szeidl, Eds. (Budapest: Konkoly Observatory, Kultura), p. 283.

BOX G.E.P., JENKINS G.M.: 1976, Time Series Analysis, forecasting and control, revised edition (San Francisco: Holden-day).

COUSINS A.W.J., LAGERWEIJ H.C., SHILLINGTON F.A.: 1969, *Mon. Notes Astron. Soc. South. Afr.* **28**, 63.

DEEMING T.J.: 1975, *Astrophys. Space Sci.* **36**, 137.

DRISSEN L., ST.-LOUIS N., MOFFAT A.F.J., BASTIEN P.: 1987, *Astrophys. J.* **322**, 888.

EDDINGTON A.S., PLAKIDIS S.: 1929, *Mon. Not. R. Astron. Soc.* **90**, 65.

EDELSON R.A., KROLIK J.H.: 1988, *Astrophys. J.* **333**, 646.

GOSSET E., VREUX J.-M., MANFROID J., STERKEN C., WALKER E.N., HAEFNER R.: 1989a, *Mon. Not. R. Astron. Soc.* **238**, 97.

GOSSET E., VREUX J.-M., MANFROID J., STERKEN C., REMY M.: 1989b, in Physics of Luminous Blue Variables, *IAU colloquium* Nr. **113**, K. Davidson, A.F.J. Moffat, and H.J.G.L.M. Lamers, Eds. (Dordrecht: Kluwer Acad. Publ.), p. 307.

HORNE J.H., BALIUNAS S.L.: 1986, *Astrophys. J.* **302**, 757.

LAFLER J., KINMAN T.D.: 1965, *Astrophys. J. Suppl. Ser.* **11**, 216.

LAMONTAGNE R., MOFFAT A.F.J.: 1987, *Astron. J.* **94**, 1008.

LOUMOS G.L., DEEMING T.J.: 1978, *Astrophys. Space Sci.* **56**, 285.

MANFROID J.: 1985, Traitement numérique des données photométriques, thèse de doctorat spécial, Université de Liège.

MANFROID J., GOSSET E., VREUX J.-M.: 1987, *Astron. Astrophys.* **185**, L7.

MANFROID J., STERKEN C.: 1987, *Astron. Astrophys. Suppl. Ser.* **71**, 539.

MCCANDLISS S.R.: 1988, On the analysis of line profile variations: a statistical approach, Ph. D. thesis, University of Colorado.

MOFFAT A.F.J.: 1977, *Inf. Bull. Var. Stars* **1265.**

MOFFAT A.F.J., NIEMELA V.S.: 1982, *Astron. Astrophys.* **108**, 326.

NEMEC A.F.L., NEMEC J.M.: 1985, *Astron. J.* **90**, 2317.

RENSON P.: 1978, *Astron. Astrophys.* **63**, 125.

SCARGLE J.D.: 1981, *Astrophys. J. Suppl. Ser.* **45**, 1.

SCARGLE J.D.: 1982, *Astrophys. J.* **263**, 835.

SCARGLE J.D.: 1989, *Astrophys. J.* (in press).

STELLINGWERF R.F.: 1978, *Astrophys. J.* **224**, 953.

STERKEN C.: 1983, *The Messenger* **33**, 10.

STROHMEIER W., KNIGGE R., OTT H.: 1964, *Inf. Bull. Var. Stars* **66.**

SWINGLER D.N.: 1989, *Astron. J.* **97**, 280.

VAN DER HUCHT K.A., VAN GENDEREN A.M., BAKKER P.R.: 1990, *Astron. Astrophys.* **228**, 108.

VAN GENDEREN A.M., VAN DER HUCHT K.A., BAKKER P.R.: 1989, *Astron. Astrophys.* **224**, 125.

VAN GENDEREN A.M., VAN DER HUCHT K.A., STEEMERS W.J.G.: 1987, *Astron. Astrophys.* **185**, 131.

WOLD H.: 1938, A Study in the Analysis of Stationary Time Series, (Uppsala: Almqvst and Wiskell).